Influence of surface interactions on spinodal decomposition

J. F. Marko
Laboratory of Atomic and Solid State Physics, Clark Hall, Cornell University, Ithaca, New York 14853-2501
(Received 16 December 1992)

Domain growth in a binary mixture, after a quench through its demixing critical point, near a boundary that attracts one of the components, is discussed. When mean-field theory is valid for equilibrium properties, a single domain may form at the substrate for much weaker surface interactions than those necessary for complete wetting in equilibrium. Prediction of a transition from such a "plating" configuration to "surface droplets" is verified using cell-dynamical simulations. At later times, if diffusion is the dominant transport process, simulations show the surface domain thickness to increase according to the bulk domain growth law $R = t^{1/3}$—if there is not *too much* order near the boundary induced by the surface forces at early times. If a series of concentration oscillations is set up near the boundary at early times, surface domain thickening can be greatly slowed down. At still later times, the role that hydrodynamic flows play in changing the surface domain size is studied: the surface tension to viscosity ratio $v_0 = \sigma/\eta$ is an upper bound on interface velocities. This bound is obeyed by recent experiments that show "fast" growth of surface domains.

PACS number(s): 68.10.Cr, 68.45.Gd, 05.70.Ln, 64.75.+g

INTRODUCTION

The equilibrium theory of wetting [1, 2] concerns the stability of coexisting phases in contact with a substrate. A basic property of such an arrangement discovered by Young in 1805 is that the contact angle that the interface between the coexisting fluid phases makes with the substrate is simply related to the surface tension between the phases σ and the difference in surface tension between the two phases and the surface $\sigma_{1,s} - \sigma_{2,s}$. Complete equilibrium wetting of the substrate by phase 2 (the removal of all 1-2 contact lines from the surface) occurs for $\sigma_{1,s} - \sigma_{2,s} > \sigma$.

Here, I examine the effect of a substrate on the nonequilibrium behavior of a mixture of two pure substances with a critical demixing phase transition at a temperature T_c. For times $t < 0$, I suppose that the mixture is at equilibrium in the one-phase region above T_c; at $t = 0$, the temperature is quenched below T_c. Thermal fluctuations will trigger "spinodal decomposition" of the unstable mixture into domains of coexisting phases [3]. In the bulk, such domains grow in size, and under a variety of conditions, the domain size grows as a power of time.

Near the surface, there are symmetry-breaking interactions since the affinities of the substrate for the two mixture components differ: these interactions are responsible for equilibrium wetting phenomena. In the nonequilibrium case, the effect of the surface interactions is enhanced by the instability of the mixture after the quench. I extend the conserved time-dependent Ginzburg-Landau (CTDGL) model (also called the Cahn-Hilliard-Cook model, or model B in the parlance of dynamic critical phenomena) [3] of phase ordering to include surface effects in Sec. I, and in Sec. II ordering at early times is discussed. The only transport mechanism in this model is diffusion.

A previous paper on this topic by Ball and Essery (BE) [4] examined the role of heat transport and nonsymmetry-breaking surface forces: they discovered that concentration waves may form, propagating from the surface into the bulk. The waves form because of conservation of each component of the mixture: an excess of component 1 at the surface requires a nearby depletion of component 1 and hence excess of component 2 some distance into the bulk; iteration of this reasoning implies a layered structure. In Sec. II I examine such phenomena in the case where the surface field explicitly breaks the symmetry of the two ordered phases. In Sec. III, thickening of the surface domains at later times via diffusion is discussed.

In Sec. IV I present results of simulations of a "cell-dynamical system" closely related to the conserved CTDGL model, including all the essential physical elements: the conservation law, thermal noise, and symmetry-breaking surface interactions. The transition between surface droplets and a single "plated" surface domain matches the scaling result of Sec. II; concentration waves similar to those studied by BE are also observed. At late times, the surface layer thickness approaches a growth law as discussed in Sec. III if the surface concentration wave structure is not too ordered. If there is a highly ordered series of concentration oscillations, the surface domains coarsen much more slowly than the bulk domains.

At late times, surface tension may drive hydrodynamic flows which cause much faster domain growth than that due to diffusion [5]. In Sec. V I consider the effect of such flows on the growth of surface domains: I find that the characteristic capillary velocity σ/η is an upper limit for interface velocities. Finally, in Sec. VI the current experimental situation is discussed.

I. MODEL FOR DIFFUSIVE PHASE SEPARATION NEAR A SURFACE

A. Equation of motion

A scalar field $\psi(\mathbf{r},t)$ is taken to represent the difference between the local concentrations of the two pure components of a binary mixture, in the region $z > 0$. Equilibrium is described by the free energy

$$\frac{F}{kT} = \int d^d r \left[\frac{\epsilon}{2}\psi^2 + \frac{u}{4}\psi^4 + \frac{c}{2}(\boldsymbol{\nabla}\psi)^2 - \sum_n \frac{1}{n}[S^{(n)}(z) + \sigma_B^{(n)}\delta(z)]\psi^n \right]. \quad (1)$$

The surface fields $S^{(n)}(z)$ are assumed to be smooth at $z = 0$; the fields $\sigma_B^{(n)}$ take into account "contact" contributions to the surface free energy. This model with only $n = 1, 2$ surface potentials is the basic model used to study equilibrium wetting phenomena [1, 2].

CTDGL dynamics of ψ take the form of a local conservation law [3]

$$\frac{\partial\psi}{\partial t} = \boldsymbol{\nabla}\cdot\mathbf{J}. \quad (2)$$

Here $\mathbf{J}$ is the total order-parameter current and is made up of two contributions. One is an average current driven by inhomogeneities in the local chemical potential $\mu(\mathbf{r}) = \delta F/\delta\psi(\mathbf{r})$; the corresponding current for small inhomogeneities is $M\boldsymbol{\nabla}\mu$, where M is a (constant) mobility. The second contribution is a stochastic current due to thermal fluctuations: each component of this current $\mathbf{j}(\mathbf{r},t)$ is taken to be a Gaussian random variable with correlations

$$\langle j_k(\mathbf{r},t) j_l(\mathbf{r}',t')\rangle = 2MkT\delta_{kl}\delta^d(\mathbf{r}-\mathbf{r}')\delta(t-t'). \quad (3)$$

The strength of the stochastic current is that required to drive the field to equilibrium where the probability of a state $\psi(\mathbf{r})$ is proportional to $\exp(-F[\psi]/kT)$.

The equation of motion for ψ is thus

$$\frac{\partial\psi}{\partial t} = M\nabla^2\mu + \eta, \quad (4)$$

where the scalar noise $\eta(\mathbf{r},t) = \boldsymbol{\nabla}\cdot\mathbf{j}(\mathbf{r},t)$ has correlations

$$\langle\eta(\mathbf{r},t)\eta(\mathbf{r}',t')\rangle = -2MkT\nabla^2\delta^d(\mathbf{r}-\mathbf{r}')\delta(t-t'). \quad (5)$$

B. Boundary conditions

Integrating ψ over the system volume yields the surface contribution

$$\frac{\partial}{\partial t}\int_V d^d r\,\psi(\mathbf{r},t) = -\hat{\mathbf{z}}\cdot\int_S d^{d-1}r\,(M\boldsymbol{\nabla}\mu + \mathbf{j}), \quad (6)$$

where S refers to the plane $z = 0$ and $\hat{\mathbf{z}}$ is the unit normal to S pointing in the $+z$ direction. Local conservation of ψ allows us to suppose that the integrand is zero. However, because of the very different short-time behaviors of the two surface contributions ($\hat{\mathbf{z}}\cdot\mathbf{j}$ and $\hat{\mathbf{z}}\cdot\boldsymbol{\nabla}\mu$), they are *each* zero at $z = 0$.

One may see this by noting that the integral of the z component of $\mathbf{j}$ over a short time τ is of order $\tau^{1/2}$ since $\mathbf{j}$ is Gaussian noise. However, the integral of the z component of $\boldsymbol{\nabla}\mu$ is of order of τ, since $\boldsymbol{\nabla}\mu$ does not vary appreciably on sufficiently short time scales. Taking τ to zero indicates that $\hat{\mathbf{z}}\cdot\mathbf{j}$ must itself vanish at $z = 0$; this in turn implies that $\hat{\mathbf{z}}\cdot\boldsymbol{\nabla}\mu = 0$ at $z = 0$. Thus there are no noise *or* diffusive currents through the surface $z = 0$.

The chemical potential μ has the form

$$\frac{\mu(\mathbf{r},t)}{kT} = \epsilon\psi + u\psi^3 - c\nabla^2\psi - \sum_n S^{(n)}(z)\psi^{n-1} - \delta(z)\left(c\hat{\mathbf{z}}\cdot\boldsymbol{\nabla}\psi + \sum_n \sigma_B^{(n)}\psi^{n-1}\right). \quad (7)$$

The terms proportional to $\delta(z)$ in (7) are due to the $(d-1)$-dimensional contact portion of the free energy. I suppose this plane to be in equilibrium with the adjacent d-dimensional bulk, or $c\hat{\mathbf{z}}\cdot\boldsymbol{\nabla}\psi + \sum_n \sigma_B^{(n)}\psi^{n-1} = 0$. This surface free-energy equilibrium condition is the same as that encountered in the equilibrium theory of wetting [1, 2]; applied to this dynamic problem, it simplifies the form of the chemical potential (7) since the contact terms vanish. This condition along with the boundary condition that the normal derivative of μ be zero, when combined with an initial condition $\psi(\mathbf{r},0)$, allow one to solve the dynamical equation (4).

C. Rescaled model

Suppose that $\epsilon = a_0$ for $t < 0$, and $-a$ for $t > 0$. In this paper changes in absolute temperature T are ignored, as they are usually small in experiments. The equation of motion and boundary conditions for ψ may be rescaled, using the transformation $\mathbf{r}/(c/a)^{1/2} \to \mathbf{r}$, $t/(c/Ma^2kT) \to t$ and $\psi/(a/u)^{1/2} \to \psi$ suggested by the characteristic distances, times, and field strengths of the $t > 0$ dynamics:

$$\frac{\partial\psi}{\partial t} = \nabla^2\left[\tau\psi + \psi^3 - \nabla^2\psi - \sum_n s^{(n)}(z)\psi^{n-1}\right] + \sqrt{g}\eta,$$

$$0 = \hat{\mathbf{z}}\cdot\boldsymbol{\nabla}\mu, \quad (8)$$

$$0 = \hat{\mathbf{z}}\cdot\boldsymbol{\nabla}\psi + \sum_n s_B^{(n)}\psi^{n-1},$$

where now $\tau = a_0/a$ for $t < 0$ and $\tau = -1$ for $t > 0$, and where $g = 2ua^{(d-4)/2}c^{-d/2}$.

The rescaled noise η has correlations in the new coordinates:

$$\langle\eta(\mathbf{r},t)\eta(\mathbf{r}',t')\rangle = -\nabla^2\delta^d(\mathbf{r}-\mathbf{r}')\delta(t-t'), \quad (9)$$

and the rescaled surface interactions take the form

$$s_B^{(n)} = a^{(n-3)/2} c^{-1/2} u^{(2-n)/2} \sigma_B^{(n)},$$
$$s^{(n)}(z) = a^{(n-3)/2} c^{-1/2} u^{(2-n)/2} \sigma^{(n)} d^{(n)}(z), \tag{10}$$
$$d^{(n)}(z) \equiv \frac{(c/a)^{1/2}}{\sigma^{(n)}} S^{(n)}([c/a]^{1/2} z),$$
$$\sigma^{(n)} \equiv \int_0^\infty dz\, S^{(n)}(z).$$

The parameter g is the familiar Ginzburg parameter, and thus the condition for mean-field bulk critical behavior for $g < 1$ translates into the low-noise limit of the rescaled dynamics [7].

I have introduced the total integrals of the finite-range surface interactions $\sigma^{(n)}$; these have the same dimensions as $\sigma_B^{(n)}$, i.e., they are surface tensions. The amplitude $\sigma^{(1)}$ is of the order of the difference between the surface tensions of the two pure components with respect to the wall, in units of kT. The normalized surface fields $d^{(n)}$ have unit integrals and allow us to see the similarities between the finite range and contact surface interactions. As can be seen from (10), the two types of surface interactions have the same dependence on the bulk parameters a, c, and u, after rescaling. When $(c/a)^{1/2}$ becomes large compared to the range of $S^{(n)}$, the functions $d^{(n)}$ become δ-function-like, and $\sigma^{(n)}$ may be absorbed into $\sigma_B^{(n)}$, altering the boundary condition that results from surface equilibrium.

II. DIFFUSIVE PHASE SEPARATION NEAR A SURFACE AT EARLY TIMES

A. Scaling behavior: Low-noise case

1. *Surface domain morphology: "Plating" vs "droplets"*

The rescaled model (8) allows us to tell when the early time (rescaled time after quench of order unity) dynamics near $z = 0$ changes from being dominated by the surface forces to being dominated by the stochastic forces. Throughout this section I assume the low-noise case where $\sqrt{g} < 1$ [6]. Suppose $s^{(n)}(z)$ is absorbed into $s_B^{(n)}$, as discussed in the preceding section; both are described by the characteristic surface tensions $\sigma_B^{(n)}$. The transition occurs for $s_B^{(n)} \approx \sqrt{g}$ or

$$\sigma_B^{(n)} \approx a^{(d+2-2n)/4} u^{(n-1)/2} c^{(2-d)/4}. \tag{11}$$

For small a, the small-n terms with rescaled amplitudes of order $s_B^{(n)}$ dominate: also, the nth-order term dominates over the noise as $a \to 0$ in dimensions larger than $d_n = 2(n-1)$. The $n = 1$ term becomes important first as a is taken to zero, and it exceeds the stochastic force for

$$\sigma_B^{(1)} > \sigma_p \approx a^{d/4} c^{(2-d)/4}. \tag{12}$$

For $\sqrt{g}$ small, the fluctuations in the initial state are small, and this transition corresponds to the point where the order parameter at the surface is driven in the direction of the symmetry-breaking surface field rather than randomly by thermal noise. Without opposing surface fields for $n > 1$, this condition should also describe the transition from surface droplets to a single domain in contact with the $z = 0$ plane. Formation of such a surface domain will be referred to as plating.

In many cases, the $n = 2$ fields oppose the formation of either ordered phase (i.e., $\sigma_B^{(2)} < 0$), due to the smaller coordination number of molecules at the surface compared to those in the bulk. If $s_B^{(2)} \ll s_B^{(1)}$, this effect may be ignored. In general, $s_B^{(1)} - s_B^{(2)} > \sqrt{g}$ is required for plating to occur.

2. *Comparison with equilbrium wetting transition: $s_B^{(1)} \gg s_B^{(2)}$*

One might ask where (in terms of distance from the critical point) the plating-droplet transition occurs relative to the equilibrium wetting transition that occurs for weak surface fields near the critical point. Equilibrium complete wetting will occur when the surface tension σ between the two coexisting phases is less than the difference in surface tensions $\sigma_{1,s} - \sigma_{2,s}$ between these two phases and the substrate [8]. Again, there are two regimes: $\sqrt{g} < 1$, where mean-field theory describes the equilbrium behavior, and $\sqrt{g} > 1$, where fluctuations qualitatively change the surface tensions of interest [2]. I again study the case $\sqrt{g} < 1$.

In the rescaled units, all bulk properties (correlation length, order-parameter scale) are of order unity, thus σ is of order 1. The difference in surface tensions between the two phases and the substrate is $\sigma_{1,s} - \sigma_{2,s} \approx s_B^{(1)}$; the criterion for complete wetting is $s_B^{(1)} > 1$. The ratio between the threshold σ_p required for plating to the threshold for equilibrium wetting is just $\sigma_p/\sigma_w \approx \sqrt{g}$.

In this case, surface forces dominate the early time dynamics near the wetting surface for much weaker surface interactions than those needed to drive complete wetting for $\sqrt{g} < 1$. In summary, for plating to occur, the symmetry-breaking field must overcome only (weak) thermal fluctuations; for equilibrium complete wetting, the difference in surface free energy of the two phases must exceed the *finite* interphase surface tension. This situation will be encountered whenever $\sqrt{g}$ is small (the quench must not be into the nonclassical scaling region).

3. *Comparison with equilbrium wetting transition: $s_B^{(1)} \approx s_B^{(2)}$*

In the case where $s_B^{(2)}$ competes with $s_B^{(1)}$, somewhat stronger symmetry-breaking surface fields are required to drive the transition to complete wetting. However, when $a \to 0$ (assuming $\sqrt{g} < 1$), the symmetry-breaking field dominates, and complete wetting occurs [2] for $\sigma_B^{(1)} > (a/u)^{1/2} \sigma_B^{(2)}$. For $\sqrt{g}$ small, this is essentially the same as the plating condition for the case where the $n = 1$ and $n = 2$ forces compete.

4. *Effect of inhomogeneity of initial state following quench*

The preceding criterion for plating is limited to cases where the initial-state fluctuations are not much more important than the surface and stochastic forces in the final state. For $a_0 > a$ this is true. In cases where mean-field theory is valid, if only the $n = 1$ surface interaction is present, the initial order-parameter profile is estimated to be $\langle \psi_k \rangle \approx s_B^{(1)}/(a_0/a + k^2)$, where ψ_k is the cosine Fourier transform of $\psi(z)$. Since I am interested in forces acting on the most unstable mode with $k \approx 1$, one observes that the initial condition never exceeds the surface force in magnitude, even for quenches with $a_0/a \approx 1$.

For highly asymmetric quenches ($a_0/a \ll 1$) there is the possibility of the dynamics at early times being dominated by "critical adsorption" of the preferred phase near $z = 0$ [9]. However, this will enhance the appearance of a surface layer near $z = 0$ for $t > 0$, and the above criterion is a lower bound as to when the surface forces to have greater effect than that of the stochastic force.

5. *Front propagation from surface following quench*

In the case where there is an extremely low level of noise in the final state, the surface field causes a front that propagates into the unstable bulk, an effect noted by BE [4] in their study of phase ordering near a surface without a symmetry-breaking surface field. This front takes the form of concentration oscillations perpendicular to the $z = 0$ plane which are damped beyond a distance of order $d = vt$, where t is time after the quench, and where v is a velocity of order unity in the rescaled units ($Ma^{3/2}kT/c^{1/2}$ in the original units).

As the front travels into the bulk, it eventually will be disturbed by concentration fluctuations originating from bulk thermal fluctuations: these grow roughly as $\langle \psi^2 \rangle \approx ge^{t/2}$ at early times (where $\langle \psi^2 \rangle \ll 1$). In rescaled units, such a front penetrates a distance w such that $\langle \psi^2(t = w/v) \rangle^{1/2} \approx s_B^{(1)}$, or $w \approx \ln(s_B^{(1)}/\sqrt{g})$ (the appearance of $s_B^{(1)}$ is discussed in Sec. II B).

Thus for very low noise levels, a series of concentration oscillations near the $z = 0$ surface may be obtained, connected to a bulk composed of random domains. Studies of the properties of these fronts, focusing on velocity selection in the low-temperature limit, have been carried out by a number of groups [4, 10]. A complete analytical calculation of the similar competition between an advancing front and thermally triggered bulk domains has been carried out in the *nonconserved* case by Mazenko, Valls, and Ruggiero [11].

B. Behavior of linearized model

If the nonlinear term in (8) is dropped, we may solve the resulting linearized model; this is valid when $|\psi| \ll 1$. The calculations of this section are similar to those of BE [4]: they are appropriate for the weak-noise case ($g \ll 1$) for times before the order parameter grows to be near unity.

In the bulk, I consider Fourier components of the order parameter $\psi_{\mathbf{k}} \equiv \int d^d r\, e^{i\mathbf{k}\cdot\mathbf{r}}$. Ignoring the surface, and dropping nonlinear terms (valid for $|\psi| \ll 1$), the equation of motion (8) is

$$\partial_t \psi_{\mathbf{k}} = -k^2(\tau + k^2)\psi_{\mathbf{k}} + \sqrt{g}\eta_{\mathbf{k}}, \tag{13}$$

where the Gaussian noise η has correlations $\langle \eta_{\mathbf{k}} \eta_{\mathbf{k}'} \rangle = k^2 \delta^d(\mathbf{k} + \mathbf{k}')\delta(t - t')$. Averaging over the noise, the equation of motion for $S_{\mathbf{k}} \equiv \langle |\psi_{\mathbf{k}}|^2 \rangle$ is

$$\partial_t S_{\mathbf{k}} = -2k^2(\tau + k^2)S_{\mathbf{k}} + gk^2. \tag{14}$$

For $\tau > 0$ (times $t < 0$ before the quench) we have the equilibrium $S_{\mathbf{k}}(0) = g/2\epsilon_k$, where $\epsilon_k \equiv \tau + k^2$. This may be used as the initial condition at $t = 0$ to obtain $S_{\mathbf{k}}$ for $t > 0$, when $\tau = -1$:

$$S_{\mathbf{k}}(t) = \frac{g}{2}\left[\frac{e^{2\sigma_k t}}{a_0/a + k^2} + \frac{k^2(e^{2\sigma_k t} - 1)}{\sigma_k}\right], \tag{15}$$

where $\sigma_k = k^2(1 - k^2)$. The most rapidly growing modes have $k = k^* = 1/\sqrt{2}$, and grow as $|\psi_{k^*}|^2 \approx ge^{t/2}$. If $g \ll 1$ and a_0/a is not too small, the field strengths ψ_k are small until a time $t \approx -\ln g$.

Near the surface, I consider the effect of the fields $s^{(1)}(z)$, $s_B^{(1)}$, and $s_B^{(2)}$. Ignoring the nonlinear term and averaging in transverse directions (eliminating derivatives in x and y and the noise) leads to an equation for the transverse-averaged order parameter $\phi(z) \equiv \int d^{d-1}r\, \psi(\mathbf{r}, t)/\int d^{d-1}r$:

$$\partial_t \phi = \partial_z^2(\tau\phi - \partial_z^2\phi - s^{(1)}). \tag{16}$$

To this are added the two $z = 0$ boundary conditions discussed in Sec. II:

$$\begin{aligned} &\partial_z \phi + s_B^{(1)} + s_B^{(2)}\phi = 0, \\ &\partial_z(\tau\phi - \partial_z^2\phi - s^{(1)}) = 0, \end{aligned} \tag{17}$$

which are applied at $z = 0$. Alternatively, these equations may be considered to be applied to $\psi(\mathbf{r}, t)$ in the noise-free case ($g = 0$).

Defining cosine Fourier transforms, e.g., $\phi_k \equiv \int_0^\infty dz \cos(kz)\phi(z)$, allows us to write the equation of motion as

$$\partial_t \phi_k = k^2(s_B^{(1)} + s_k^{(1)} - \epsilon_k \phi_k) + \frac{2s_B^{(2)}k^2}{\pi}\int_0^\infty dk \phi_k. \tag{18}$$

The symmetry-breaking contact and longer-ranged surface interactions have very similar effects. The $n = 2$ contact force couples modes with different k, and to simplify the calculations I will set $s_B^{(2)} = 0$ to focus on the effect of the symmetry-breaking ($n = 1$) fields.

For $t < 0$, the equilibrium solution is $\phi_k(0) = [s_k^{(1)} + s_B^{(1)}]/\epsilon_k$. In the case of a short-ranged surface interaction, $s_k = 0$, and thus the real-space adsorption is $\phi(z, t < 0) = (s_B^{(1)}/\tau^{1/2})e^{-\tau^{1/2}z}$. This result is valid so long as $s_B^{(1)}/\tau^{1/2} \ll 1$. Using the more general result $\phi_k(0)$ as an

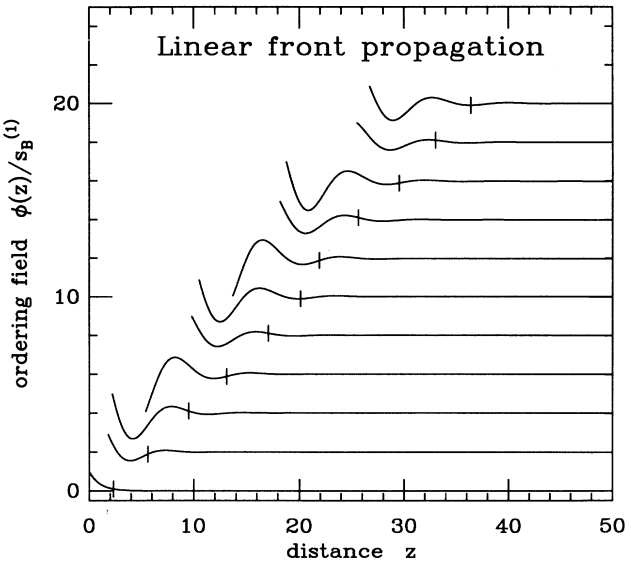

FIG. 1. Front propagation in linearized model of Sec. II B. Plotted from bottom to top are $\phi(z,t)/s_B^{(1)}$ for times $t = 0$, 2, 4, . . ., 20 (t is added to each curve to offset them). The ticks show where $|\phi/s_B^{(1)}|$ first exceeds 0.1 at each time, indicating a front velocity of about 1.7.

initial condition, the $t > 0$ evolution of ϕ_k is

$$\phi_k(t) = [s_k^{(1)} + s_B^{(1)}]\left(\frac{e^{\sigma_k t}}{a_0/a + k^2} + \frac{e^{\sigma_k t} - 1}{\sigma_k}\right). \quad (19)$$

As in the bulk, the fastest growing modes have $k = k^* = 1/\sqrt{2}$, and grow as $\phi_{k^*}(t) \approx [s_{k^*}^{(1)} + s_B^{(1)}]e^{t/4}$. In Fig. 1 $\phi(z,t)/s_B^{(1)}$ is shown for the case $s_k^{(1)} = 0$ and $a_0/a = 1$; a front that propagates away from $z = 0$ at a velocity of order unity is observed. Nonlinearities cause selection of a different front velocity, but it will be of order unity in the rescaled units [4, 10].

III. DIFFUSIVE LATE-STAGE SURFACE GROWTH

1. *Diffusive bulk domain growth*

At late times, one can adopt a scaling description of the growth of the bulk domains [12] as their interiors approach the equilibrium concentrations $|\psi| = \psi_0$. The free energy density is of order $\mu\psi_0$. If the bulk domains have a characteristic size $R(t)$, local variations in free-energy density are to be of order of the interfacial energy per unit volume $\mu\psi_0 \approx \sigma/R$, where σ is the surface tension between the ordered phases. The gradients of chemical potential are of order $\nabla\mu \approx \sigma/(\psi_0 R^2)$, and drive currents $j \approx M\nabla\mu$. The flux of order parameter thus created across a boundary causes it to move with a velocity of order $dR/dt \approx j/\psi_0 \approx M\sigma/(\psi_0^2 R^2)$, which leads to the "Lifshitz-Slyozov" or diffusive growth law $R(t) \approx (M\sigma t/\psi_0^2)^{1/3}$, where ψ_0 is the value of the saturated ordering field.

2. *Diffusive thickening of surface layer*

This approach may be used to estimate the growth law for a surface layer in contact with bulk domains. Suppose that the surface layer is a thickness $h(t)$ and that there are bulk domains characterized by a scale $R(t)$ a distance of order $R(t)$ above the surface. Again, since the surface domains are very flat and thus have a small amount of interface energy stored per unit volume, I conclude that the gradients of μ in the region between the bulk and surface domains are just $\nabla\mu \approx \sigma/(\psi_0 R^2)$. Thus the rate of growth of the surface layer will be $dh/dt \approx M\sigma/(\psi_0^2 R^2)$; the known behavior of $R(t)$ leads to the scaling law $h(t) = R(t)$. Alternatively, if the thickness of the "depletion" region between the surface layer and the bulk domains is of order $h(t)$, then $\nabla\mu \approx \sigma/(\psi_0 Rh)$. This leads to the growth equation $dh/dt \approx M\sigma/(\psi_0^2 Rh)$, which again gives the scaling result $h(t) = R(t)$ when the explicit bulk result for $R(t)$ is adopted [13].

3. *Stability of plated structure under partial wetting conditions*

As the surface layer thickens, if the equilibrium wetting state is partial wetting, one might ask how likely it is for an interfacial fluctuation to occur that punches a hole through the metastable surface film. Since such a fluctuation requires an amount of surface area of order h^{d-1} to be created, the associated activation barrier grows with time as $E_{\rm act} \approx \sigma h^{d-1} \propto t^{(d-1)/3}$. The number of possible sites for such a hole is of order $(S/h)^{d-1}$, where S is the characteristic length of the sample. The total rate at which these fluctuations will be activated therefore decreases with time as $S^{d-1}t^{-(d-1)/3}\exp(-t^{(d-1)/3})$, suggesting that a plated surface quickly becomes very stable. This rate estimate also suggests that at late times, stability of plating increases with space dimension. It would be useful to better understand the time scale for a plated surface layer to relax to a partially wetting configuration: this will depend sensitively on the rate at which surface fluctuations grow in amplitude on the (moving) surface domain wall. The simulation results of Sec. IV indicate that this time can be very long: however, as yet I do not have a convincing estimate for it.

4. *Mullins-Sekerka instability of surface domain*

We have seen that a plated surface layer should asymptotically thicken at the same rate as the bulk domains. Thus I envision a flat interface moving at a velocity $v = dR/dt \approx (M\sigma/\psi_0^2)t^{-2/3}$. Since the process by which material is transported into the surface layer parallels the diffusion of heat or impurities from a moving solid-liquid interface, one might ask whether there is a Mullins-Sekerka instability in our case. In fact, the "chemical model" formalism of Langer [14] can be directly applied to this problem, resulting in a prediction of a characteristic wavelength $\lambda^* \approx \sqrt{2Dd_0/v}$, where D is the diffusion constant ($D = kTMa$ in the unrescaled mean-field theory) and $d_0 = \sigma/(kTa\psi_0^2)$ is the appropriate mean-field capillary length (ratio of surface tension to total free-

energy density of the ordered phase). The interface is unstable to fluctuations in the interface at a scale longer than λ^*.

The scaling result for the interface velocity $v = dR/dt$ leads to $\lambda^* \approx R(t)$. It is thus likely at late times for the surface layer to develop corrugations at the scale of the bulk ordering wavelength. Of course, fluctuations in the diffusing field due to the bulk pattern will interfere with the diffusing field at scales of λ^*, and the simple theory (for a flat interface entering a featureless medium) is inapplicable. Nevertheless, this calculation is useful since it indicates that the Mullins-Sekerka mechanism *does not* introduce a new length scale for transverse structure of growing surface domains that is smaller than $R(t)$.

IV. SIMULATIONS

In Sec. I, by rescaling space, time, and field strength, all parametric dependence of phase ordering near a surface was moved into the surface potentials and the noise strength. This suggests a transition for the surface ordering from a noise-dominated to a noiseless (zero-temperature) regime. A hypothesis about the long-time behavior of surface domains in the two regimes was that in the former, noisy, case, one observes domains of both phases in contact with the surface; in the latter, one observes only the attracted phase in a plated morphology with no domain walls at $z = 0$. In this section, I check this hypothesis, by numerically integrating phase-ordering dynamics for different strengths of noise and surface force.

In order to study the dynamics of (8) I have used two- and three-dimensional cell-dynamical systems (CDS's) [15], which may be roughly considered to be a discretization of the partial differential equations of Sec. I. Space and time are discretized, and periodic boundary conditions are used in the x direction in the two-dimensional case and in the x and y directions in the three-dimensional case. The x, y, and z positions run from $1/2$ to $N_x - 1/2$, $N_y - 1/2$, and $N_z - 1/2$ in steps of 1, respectively. Impenetrable surfaces with identical surface interactions at $z = 0$ and $z = N_z$ are considered. Our model is an extension of one due to Oono and Puri, and I follow their notation [15].

A. Cell dynamics for $d = 2$

The following iteration rule may be adopted for the ordering field $\psi(x,z,t)$, where time t is an integer:

$$\begin{aligned}\psi(x,z,t+1) = \psi(x,z,t) \\ -R(\langle\langle m[\psi(x,z,t)]\rangle\rangle - m[\psi(x,z,t)]) \\ +\sqrt{G}N(x,z,t),\end{aligned} \tag{20}$$

where the "map" m is defined to be

$$\begin{aligned}m[\psi] = A\psi/\sqrt{1+(A^2-1)\psi^2} \\ +s(z)\ln A - \psi + D[\langle\langle\psi\rangle\rangle - \psi],\end{aligned} \tag{21}$$

where $s(z)$ is the one-body surface field ($s^{(1)}$) of (8) and where the averaging operator $\langle\langle\,\rangle\rangle$ is defined for any function $F(x,z)$:

$$\begin{aligned}\langle\langle F(x,z)\rangle\rangle \equiv [F(x+1,z)+F(x-1,z)+F(x,z-1)+F(x,z+1)]/6 \\ +[F(x+1,z+1)+F(x+1,z-1)+F(x-1,z+1)+F(x-1,z-1)]/12.\end{aligned} \tag{22}$$

These dynamics require $m(x,z,t)$ and $\psi(x,z,t)$ for $z = -1/2$ and $z = N_z + 1/2$: boundary conditions on these fields can be used to supply these values. Discretizing $\hat{\mathbf{z}}\cdot\nabla\psi = 0$ and $\hat{\mathbf{z}}\cdot\nabla m = 0$ gives

$$\begin{aligned}\psi(x,-1/2,t) &= \psi(x,1/2,t), & \psi(x,N_z+1/2,t) &= \psi(x,N_z-1/2,t), \\ m(x,-1/2,t) &= m(x,1/2,t), & m(x,N_z+1/2,t) &= m(x,N_z-1/2,t).\end{aligned}$$

The condition on ψ corresponds to $s_B^{(n)} = 0$: this is easily altered to take into account nonzero contact forces. In this section, surface forces are studied using the field $s(z)$ which corresponds to $s^{(1)}(z)$ in (8): the other fields $s^{(n)}(z)$ coupled to ψ^{n-1} are easily included.

The scalar noise N is defined at our lattice sites in terms of currents $\{\theta_1,\theta_2\}$:

$$\begin{aligned}N(x,z,t) = [\,\theta_1(x+1/2,z,t) - \theta_1(x-1/2,z,t) \\ +\theta_2(x,z+1/2,t) - \theta_2(x,z-1/2,t)],\end{aligned} \tag{23}$$

where the θ's are Gaussian random variables with the correlations

$$\langle\theta_k(x,z,t)\theta_{k'}(x',z',t')\rangle = \delta_{k,k'}\delta_{x,x'}\delta_{z,z'}\delta_{t,t'}. \tag{24}$$

The currents can be thought of as lying on the bonds between the order-parameter sites. The currents through the boundaries vanish [$\theta_2(x,0,t) = \theta_2(x,N_z,t) = 0$] in accord with the surface condition $\hat{\mathbf{z}}\cdot\mathbf{j} = 0$.

For $t < 0$, similar dynamics may be used, replacing the map defined above with

$$\begin{aligned}m_0[\psi] = \frac{Q^{1/2}A^{-Q}\psi}{\sqrt{Q+(1-A^{-2Q})\psi}} \\ +s(z)\ln A - \psi + D[\langle\langle\psi\rangle\rangle - \psi].\end{aligned} \tag{25}$$

For $A \to 1+$, the CDS reduces to Euler integration of the nonlinear partial differential equation (8) with the $n = 1$ surface force, boundary conditions, and noise as defined in (8), and with an (order unity) mobility constant M:

$$\partial_t\psi = M\nabla^2[\tau\psi + \psi^3 - \nabla^2\psi - s(z/\Delta_x)] + \sqrt{g}\eta, \tag{26}$$

where $\tau = Q$ for $t < 0$ and $\tau = -1$ for $t > 0$. In this limit,

Q is a_0/a of (8), the time steps are (in the units of the differential equation) $\Delta_t = A - 1$, the spatial grid has a lattice constant of $\Delta_x = (3\Delta_t/D)^{1/2}$, the noise strength of the differential equation is $g = G(\Delta_x)^{2+d}/\Delta_t$, and $R = (3M/\Delta_x^2)$. This limit also indicates that m plays the role of the chemical potential of the continuum Landau-Ginzburg model.

I have chosen the parameters used by Oono and Puri [15]: $R = 1$, $A = 1.3$, and $D = 0.7$. The time step is thus about 0.3 and the lattice constant is of order 1.1 in the units of the partial differential equation (PDE). The fact that a discrete mapping can be defined with such a large time step motivates the use of the CDS rather than direct integration of the nonlinear PDE. Another favorable property of the CDS is that it is very stable in the presence of moderately large external fields ($s \approx 0.5$). The noise strength G and the surface fields $s(z)$ of the CDS can be taken to be the parameters g and $s^{(1)}(z)$ up order-unity prefactors.

I have examined two types of surface interactions: a short-range "δ-function" interaction $s(z) = H\delta_{z,1/2}$ and a long-range "van der Waals" interaction $s(z) = H(1 + [z - 1/2]^3)^{-1}$. These interactions are applied near the surface $z = N_z$ as well. In each case, the sum $\sum_z s(z) \approx 1$, and so H is of order the total integrated surface potential ($s_B^{(1)}$ of Sec. I). The surface field strength H and the noise strength G thus describe the $t > 0$ model; in addition, the parameter Q completes the description of the model for $t < 0$.

B. Cell dynamics for $d = 3$

The two-dimensional model described in the preceding subsection is easily extended to $d = 3$, to the geometry where there are two parallel zero-flux surfaces at $z = 0$ and $z = N_z$. The iteration rule (20), the maps (21), and (25), and the boundary conditions (23) are unchanged apart from the addition of the y coordinate. The noise source requires the addition of another Gaussian field θ_3.

The averaging operator of Oono and Puri for $d = 3$ is used,

$$\begin{aligned}\langle\langle F(x,z)\rangle\rangle \equiv \{&6[F(x+1,y,z)+\cdots]\\ &+3[F(x+1,y+1,z)+\cdots]\\ &+[F(x+1,y+1,z+1)+\cdots]\}/80.\end{aligned} \tag{27}$$

In this case, the time step is $\Delta_t = A - 1$, the lattice constant is now $\Delta_x = (40\Delta_t/11D)^{1/2}$, $R = 40M/(11\Delta_x^2)$, and $g = G(\Delta_x)^{2+d}/\Delta_t$. Again, $D = 0.7$, $A = 1.3$, and $R = 1$ in these calculations, which corresponds to $\Delta_t = 0.3$ and $\Delta_x = 1.25$.

C. Zero-temperature equilibrium wetting behavior

With $G = 0$ one can observe the zero-temperature transition from partial to complete wetting for droplets in contact with the active surfaces using the rescaled model for $t > 0$: as expected, this occurs for $H \approx 1$. This transition can be predicted using the continuum free-energy density

$$\mathcal{F}[\psi] = \frac{1}{2}(\nabla\psi)^2 - \frac{1}{2}\psi^2 + \frac{1}{4}\psi^4 - s(z/\Delta_x)\psi \tag{28}$$

by calculating the surface tensions. The surface tension between the two phases may be computed from the zero temperature "kink" solution to the equilibrium condition in the bulk, $-\psi_0 + \psi_0^3 - \nabla^2\psi_0 = 0$. The solution is simply

$$\psi_0(x) = \tanh x/\sqrt{2}. \tag{29}$$

The surface tension is just

$$\sigma = \int_{-\infty}^{+\infty} dx \left[\frac{1}{2}(\nabla\psi_0)^2 - \frac{1}{2}\psi_0^2 + \frac{1}{4}\psi_0^4\right], \tag{30}$$

which yields $\sigma = 2\sqrt{2}/3 = 0.9428\ldots$.

The difference in surface tensions between the two ordered phases and the substrate is

$$\sigma_{1,s} - \sigma_{2,s} = \int_0^\infty dz(\mathcal{F}[\psi_+] - \mathcal{F}[\psi_-]), \tag{31}$$

where $\psi_\pm(z)$ are solutions to $\mu(z) = 0$ connecting to $\psi(z) = \pm 1$ at $z \to \infty$. A lowest-order estimate of these solutions is $\psi_\pm = \pm 1$, giving

$$\sigma_{1,s} - \sigma_{2,s} = 2\int_0^\infty dz\, s(z/\Delta_x) = 2\Delta_x \int_0^\infty dx\, s(x). \tag{32}$$

For the two types of surface interactions studied, (a) $s(x) = H\Theta(1 - x)$ where $\Theta(x)$ is the unit step function and (b) $s(x) = H/(1+x^3)$, the surface tension differences are

$$\begin{aligned}&\text{(a) } \sigma_{1,s} - \sigma_{2,s} = 2\Delta_x H,\\ &\text{(b) } \sigma_{1,s} - \sigma_{2,s} = \frac{4\pi}{3\sqrt{3}}\Delta_x H. \approx 2.4\Delta_x H.\end{aligned} \tag{33}$$

For the discrete CDS, a better estimate of $\sigma_{1,s} - \sigma_{2,s}$ for case (b) is the sum

$$\sigma_{1,s} - \sigma_{2,s} = 2\Delta_x H \sum_{z=0,1,2,\ldots} \frac{1}{1+z^3} \approx 3.4\Delta_x H. \tag{34}$$

Young's law states that the equilibrium wetting angle θ_W should be determined by [1] $\cos\theta_W = (\sigma_{1,s} - \sigma_{2,s})/\sigma$. For $d = 2$ where $\Delta_x = 1.1$, the two types of surface interactions yield (a) $\cos\theta_W \approx 2.3H$ and (b) $\cos\theta_W \approx 4.0H$. Thus complete wetting should occur for (a) $H > 0.44$, and (b) $H > 0.25$.

As an example of the use of this criterion, I have determined the zero-temperature wetting behavior of the δ-function potential [case (a) above; in the CDS it is of course a step-function potential] for $d = 2$. A small system with $N_x = 128$ and $N_z = 32$ was studied, with an initial condition consisting of a 32-cell wide band of the preferred phase: $\psi(x,z,t=0) = +1$ for $48 < x < 80$ and $\psi(x,z,t=0) = -1$ otherwise. The zero-noise CDS was applied to this state and an equilibrium state was obtained. The equilibrium interface shape extracted from the zero-crossing points of the final field configuration for various H is shown in Fig. 2. As H is increased, the contact angle is reduced. For $H > 0.5$ complete wetting

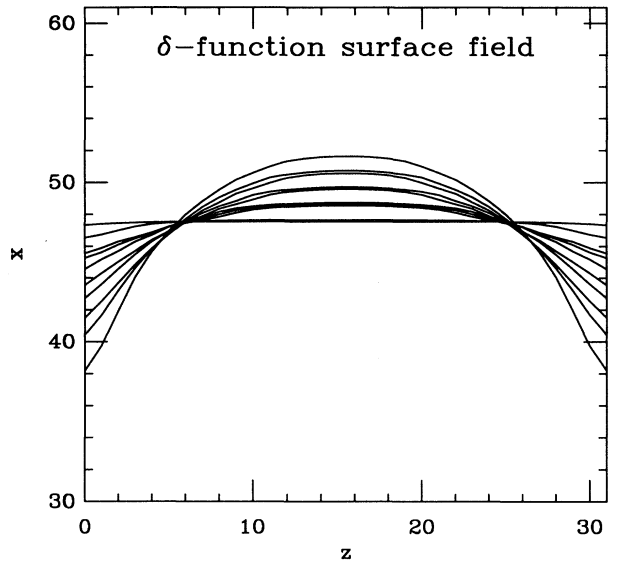

FIG. 2. Equilibrium interfaces showing contact angles for δ-function surface interactions. Interfaces for $H = 0.05$, 0.1, 0.15, 0.2, 0.25, 0.3, 0.35, 0.4, 0.45, and 0.5 are shown. The wetting surfaces are at $z = 0$ and $z = 31$; the x coordinate runs from 0 to 127.

occurs, close to our estimate of 0.44.

In Fig. 3 the contact angles extracted from the interfaces of Fig. 2 are compared to the continuum estimate $\theta_W = \cos^{-1} 2.3H$ (the contact angles were extracted by fitting the interfaces to circles). We see that there is close agreement for small H, but for $H > 0.3$ the simulation contact angles are somewhat larger than those predicted by the simple estimate above. This is likely due to neglect

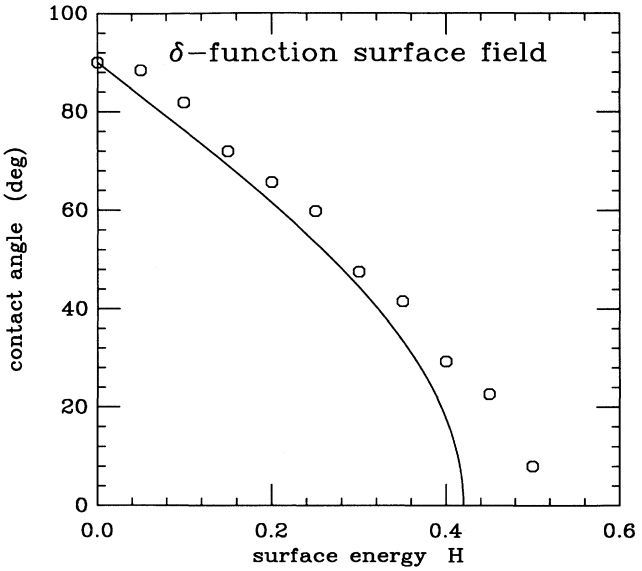

FIG. 3. Circles indicate the contact angles derived from the interfaces of Fig. 2. Solid line is the estimate based on analysis of the continuum model.

of deformation of the uniform states $\psi_\pm$ by the surface potential.

Similar agreement between the above estimate and the CDS was found using the van der Waals potential (b). The agreement between the continuum estimate and these crude measurements indicates that the CDS has a zero-temperature wetting transition at a value of H in reasonable agreement with that of the continuum model.

D. Exchange of dominance of noise and surface force at early times

I have checked the scaling prediction $\sqrt{G} \approx H$ of a transition in the late-time morphology from surface plating to isolated surface droplets in contact with the surface at the equilibrium contact angle. Our studies have been of 64×64 cell systems, with equilibration for 256 time steps before $t = 0$, with $Q = 1$. Following this initial equilibration, I have studied the evolution of the $t > 0$ dynamics for up to 50 000 time steps. After ≈ 400 steps, the morphology is stable, and runs to $t = 1024$ were used to determine the late-time morphology.

The late-time morphology was determined by counting the number of boundary sites for which $\psi < 0$: if there are none, the morphology is considered to be plated, while if there are any sites with $\psi < 0$, the morphology is considered to be "surface droplets." At late times, such sites always indicate regions of nonpreferred phase in contact with the surface. Figure 4 shows a series of final states similar to those used for this study, for $G = 0.01$, and with $H = 0.1$, 0.2, 0.4, and 0.6. For $H = 0.1$ and 0.2, interfaces between the two phases are in contact with the surfaces $z = 0$ and $z = 64$. However, for $H = 0.4$ and 0.6, we find a plated morphology: $\psi > 0$ next to the surfaces $z = 0$ and $z = 64$. In this case ($G = 0.01$), the change from surface droplet to plated morphology occurs at about $H = 0.25$.

Figure 5 indicates the plating-droplet transition for $d = 2$ and $d = 3$: over a large range of G and H, the scaling prediction of $G \approx H^2$ holds. The transitions are numerically almost the same in two and three dimensions, in agreement with the scaling argument. This behavior is insensitive to the initial conditions: runs that use an initially homogeneous initial condition ($\psi = 0$) lead to the same results.

E. Scaling behavior of ordering at late times

The bulk pattern at late times may be studied using the real-space correlator defined in the x direction:

$$g(x,t) = N_x^{-1} \sum_{x'} N_z^{-1} \sum_{z,z'} \phi(x',z,t)\phi(x'+x,z',t), \tag{35}$$

which corresponds to the Fourier transform of the scattering function that would be experimentally observed in elastic scattering with momentum transfer in the x direction. This function is dominated by the bulk and an oscillating behavior of $g(x,t)$ is observed; as $x \to \infty$,

$g \to 0$. The location of the first zero of $g(x)$ indicates the domain size $R(t)$; we observe this to increase for $t > 500$ roughly as $t^{1/3}$ in the absence of noise and surface forces, as reported by Oono and Puri [15].

At late times for the plated morphology, one can measure the thickness of the surface layer by finding the z position $h(t)$ of the first zero of the z-order parameter profile:

$$\phi(z,t) = N_x^{-1} \sum_x \psi(x,z,t). \tag{36}$$

In Fig. 6, the evolutions of the two lengths $R(t)$ and $h(t)$ are shown for three cases using the δ-function surface potential, $Q = 1$, $H = 0.2$, and (a) $G = 10^{-2}$, (b) 10^{-4}, and (c) 10^{-8}. Each of these results is obtained from averaging of results of six runs using different pseudorandom numbers. In each of these cases, equilibrium partial wetting is expected since the Ginzburg parameter $G \ll 1$ and the surface field is well below the zero-temperature complete wetting threshold $H < 0.5$.

In case (a), h and R grow at almost the same rate [Fig. 6(a)] and for times beyond 3000 ($\ln t > 8$) approach

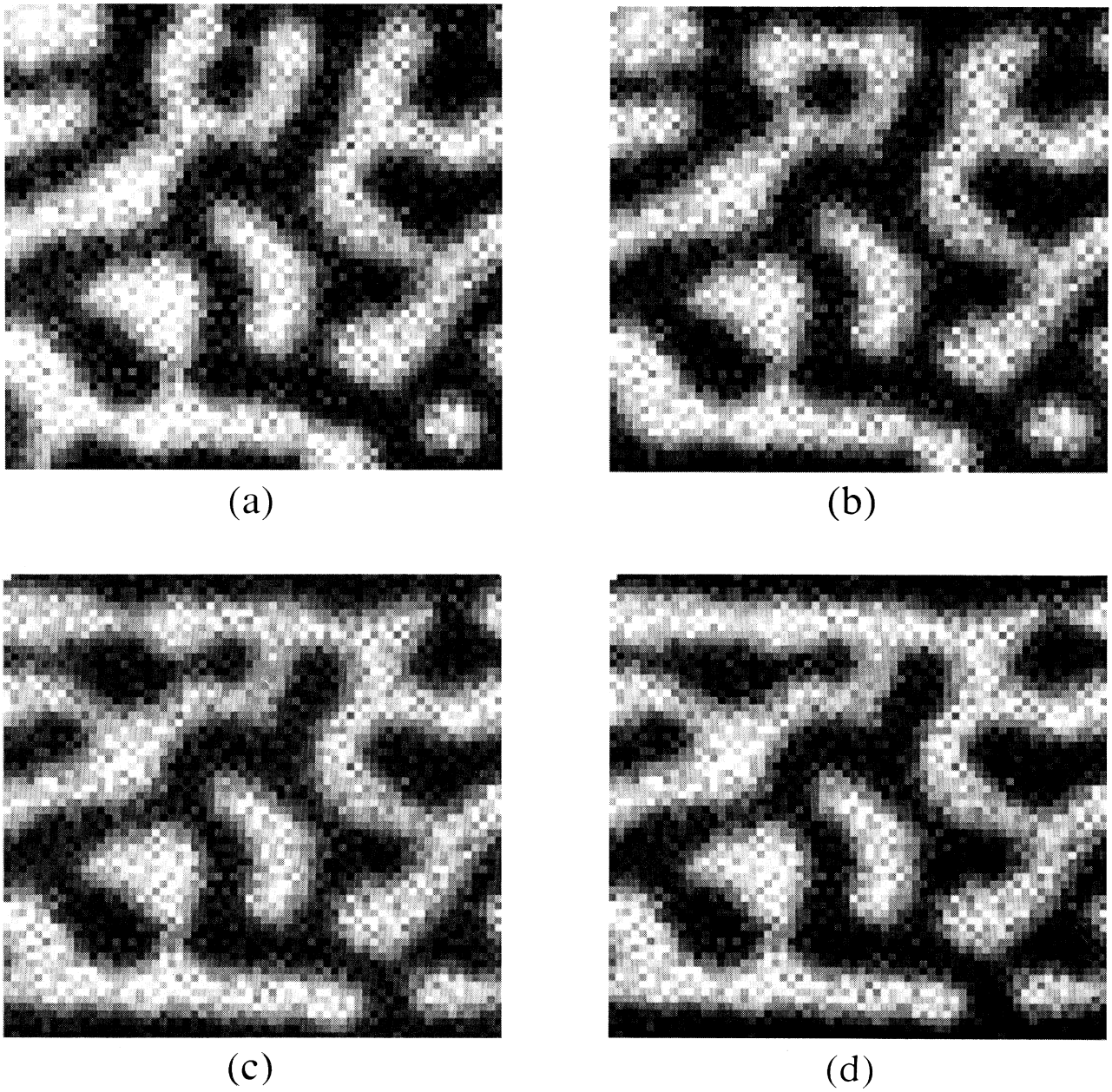

FIG. 4. Configurations of 64×64 CDS at time $t = 1024$ for $G = 0.01$ and $H = 0.1$, 0.2, 0.4, and 0.6 are shown in (a), (b), (c), and (d), respectively. The wetting surfaces are at the top and bottom of the figures. Cases (a) and (b) show surface droplets; (c) and (d) show "plating."

$t^{1/3}$. In Fig. 7(a), I show $\psi(x,z)$ at $t = 1024$: the bulk pattern is seen to extend to within $2R$ or so of the wetting surfaces. Figure 8(a) shows the $\phi(z)$ plotted at a series of times: the surface concentration waves penetrate only about a wavelength into the bulk, where the random pattern begins. In this case, transport of material to the surface is very similar to transport in the bulk. Brown and Chakrabarti have recently reported $t^{1/3}$ growth of a surface domain using a discretized Langevin equation in two dimensions [16]: they choose parameters that result in the development of a single surface domain in contact with a random bulk domain pattern similar to that shown in Fig. 7(a).

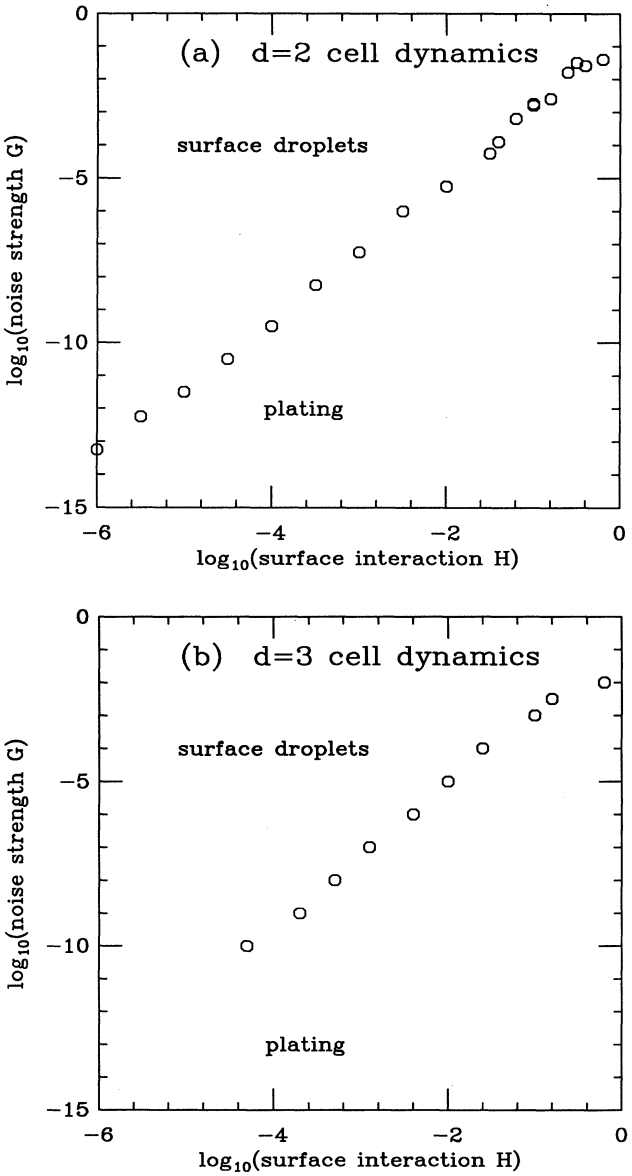

FIG. 5. Transition from plating to surface droplet morphology. Results for $d = 2$ and $d = 3$ are shown in (a) and (b), respectively. The transition line is well fit by $G = H^2$ over a very wide range.

In the lower-noise case (b), Fig. 6 shows that the bulk growth continues to behave as $R \approx t^{1/3}$ at late times, but that the surface domain thickness h lags considerably behind R. With still lower levels of noise [Fig. 6(c)], the bulk domains continue to grow as $R \approx t^{1/3}$ at late times, but now the surface domain is growing at an extremely slow rate over the times simulated ($t < 50\,000$). This slowing down may be understood at a qualitative level by observing Figs. 8(b) and 8(c): these plots of $\phi(z)$ show that as the noise level is reduced, the concentration waves penetrate further to larger values of z before they are stopped by the random pattern that is triggered by random fluctuations. Recall the estimate for the thickness of the parallel waves of order $w \propto \ln(H/G^{1/2})$; using a prefactor of 3 leads to an estimate of $w \approx 9$, 18, and 36 in cases (a), (b), and (c), which gives a good estimate of the distance that the concentration waves propagate out to in Fig. 8.

Plots of a configuration at $t = 1024$ for these cases are shown in Figs. 7(b) and 7(c). The concentration waves order the region near the surface at very early times ($t < 300$), but at very low noise levels, the resulting very clean, periodic structure coarsens slowly at later times, likely because the routes to shifts of the ordering wavelength near the surface involve large increases in local free energy. In the lowest-noise case, $G = 10^{-8}$, Fig. 8(c) shows that there is almost no change in the structure of the domain attached to the surface over the course of the simulation.

Figure 8(c) also indicates how relaxation in the low-noise cases will eventually occur: at $t = 512$ there are four concentration peaks that approach $\phi(z) = 1$, the saturated limit. At $t = 1024$, the second and third peak of $\phi(z)$ are coalescing: Fig. 7(c) shows $\phi(x,z)$ at that time. By $t = 2048$, Fig. 7(c) shows that this coalesence is complete, since the second peak in $\phi(z)$ is nearly saturated and occurs between the second and third peak positions at time $t = 512$. At later times, the shape of $\phi(z)$ near $z = 0$ begins to change, accompanied by a gradual decay of the second peak which indicates the invasion of the surface pattern by the randomly oriented bulk domains.

This suggests an estimate for the time that the surface domain growth will lag over the bulk growth since the $t^{1/3}$ coarsening can only occur when the surface domain is adjacent to inhomogeneities [as in case (a) and in the latter stages of case (b)]. This will require at least a time $T \approx w^3$ to occur, the transport time across the distance w that the concentration waves initially propagate. In cases (a), (b), and (c), these times are of order 800, 6000, and 45 000.

In Fig. 9, R and h are shown for the case $G = 0.01$ and $H = 0.4$. The effect of increasing the surface field at fixed noise strength [compare Figs. 6(a) and 9] is similar to that of decreasing the noise at fixed surface field [compare Figs. 6(a) and 6(b)]: in either case at late times the length h lags behind R due to the formation of a more ordered surface wave structure at early times.

A similar study using the van der Waals surface potential was done: the results are similar. No significantly different late-time behavior is observed: the main dif-

ference is that at early times the remnant of the $t < 0$ high-temperature adsorption extends to larger distances z due to the long tail of the surface potential.

V. HYDRODYNAMIC EFFECTS ON SURFACE STRUCTURE AT LATE TIMES

A. Flow-driven growth of bulk domains

At late times in fluid mixtures in three dimensions, growth kinetics may be dramatically altered by surface-tension-driven hydrodynamic flows. A scaling theory for such growth may be constructed from the equation for dissipative (Stokes) flow [5]

$$\eta \nabla^2 v = \nabla p, \tag{37}$$

where v is the fluid velocity, η is the viscosity, and p is the hydrostatic pressure. In the bulk, I suppose that $v \approx dR/dt$, the interface velocity; p is estimated as $\mu \approx \sigma/R$ (this is the interface energy per unit volume), and thus ∇p is taken to be of order σ/R^2. Therefore $dR/dt \approx \sigma/\eta$. The resulting growth law $R \approx v_0 t$ dominates over

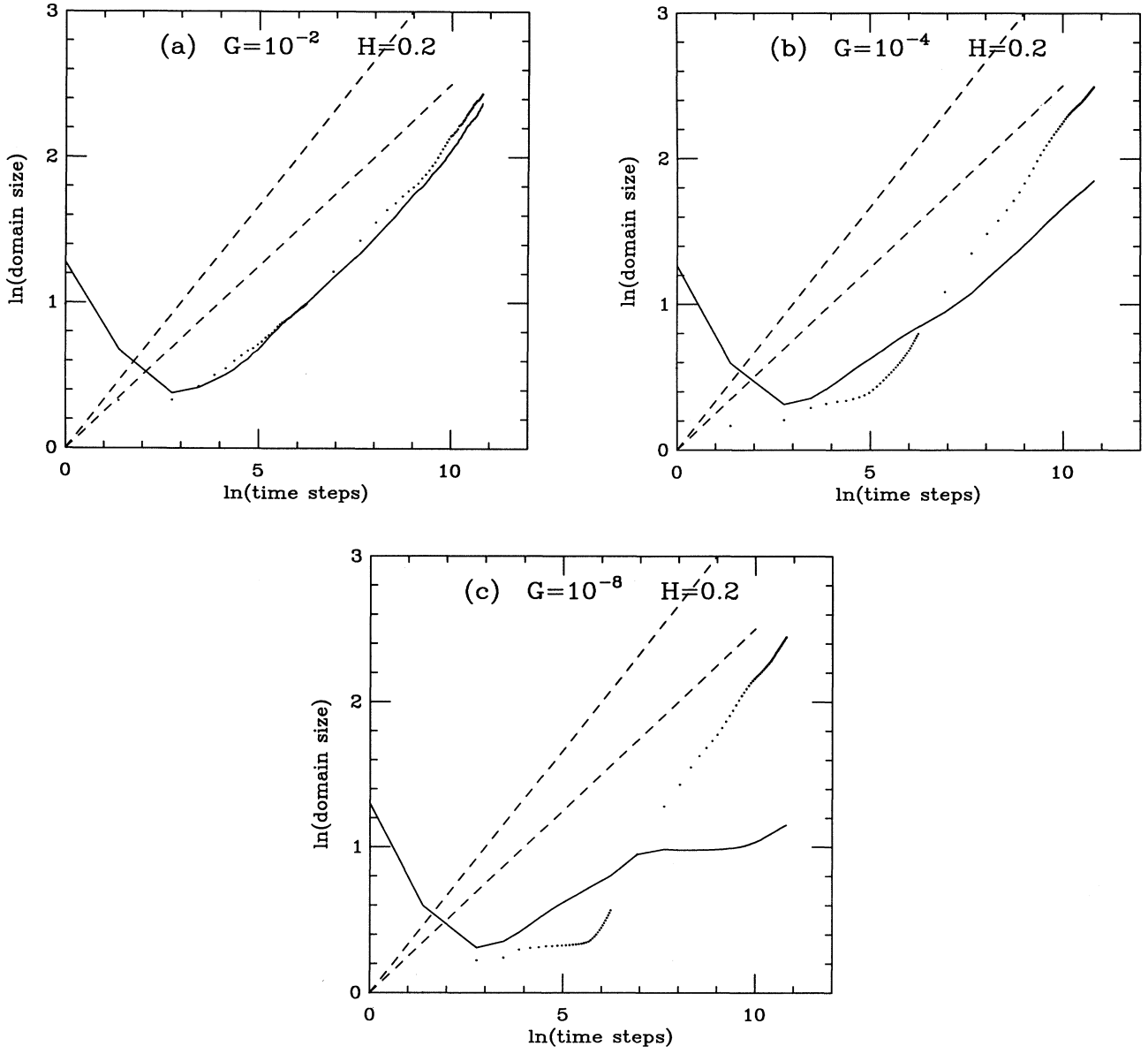

FIG. 6. Bulk domain scale $R(t)$ and surface domain thickness $h(t)$, for δ-function surface fields with $H = 0.2$. In each case, the dots indicate $R(t)$ and the solid line indicates $h(t)$, while the two dashed lines show the power laws $t^{1/3}$ and $t^{1/4}$. The largest times are $t = 50\,000$; the three cases differ only in the noise strength G used. (a) $G = 10^{-2}$: bulk and surface domain scales are comparable, and approach $t^{1/3}$, at late times. (b) $G = 10^{-4}$: bulk domains coarsen faster than surface domain thickens. Surface domain thickness is not yet approaching $t^{1/3}$ as late as $t = 50\,000$. (c) $G = 10^{-8}$: bulk domains approach $t^{1/3}$ growth at late times, while almost no surface domain thickening occurs beyond $\ln t \approx 7$.

the diffusive coarsening law ($t^{1/3}$) at late times. The characteristic velocity $v_0 = \sigma/\eta$ will play a central role in this section.

In what follows, I estimate the rate of incorporation of small droplets into a much larger one (possibly a surface layer) via flows driven by capillary forces: my motivation is to understand how the diffusive surface domain growth laws are affected by these flows. I first consider a simple problem of coalescence of a single bulk domain and a surface layer, then I use the result to study the experimentally relevant case of many bulk domains being absorbed by a surface domain. Finally, I consider spreading of surface domains in contact with bulk domains. In each case, v_0 emerges as the characteristic velocity for flows, and thus for interface motion near surfaces.

B. Incorporation of one bulk domain into a surface layer

We begin with a simple problem: an estimate of the time required for a single small droplet to flow into a large surface domain. Suppose that the small droplet is

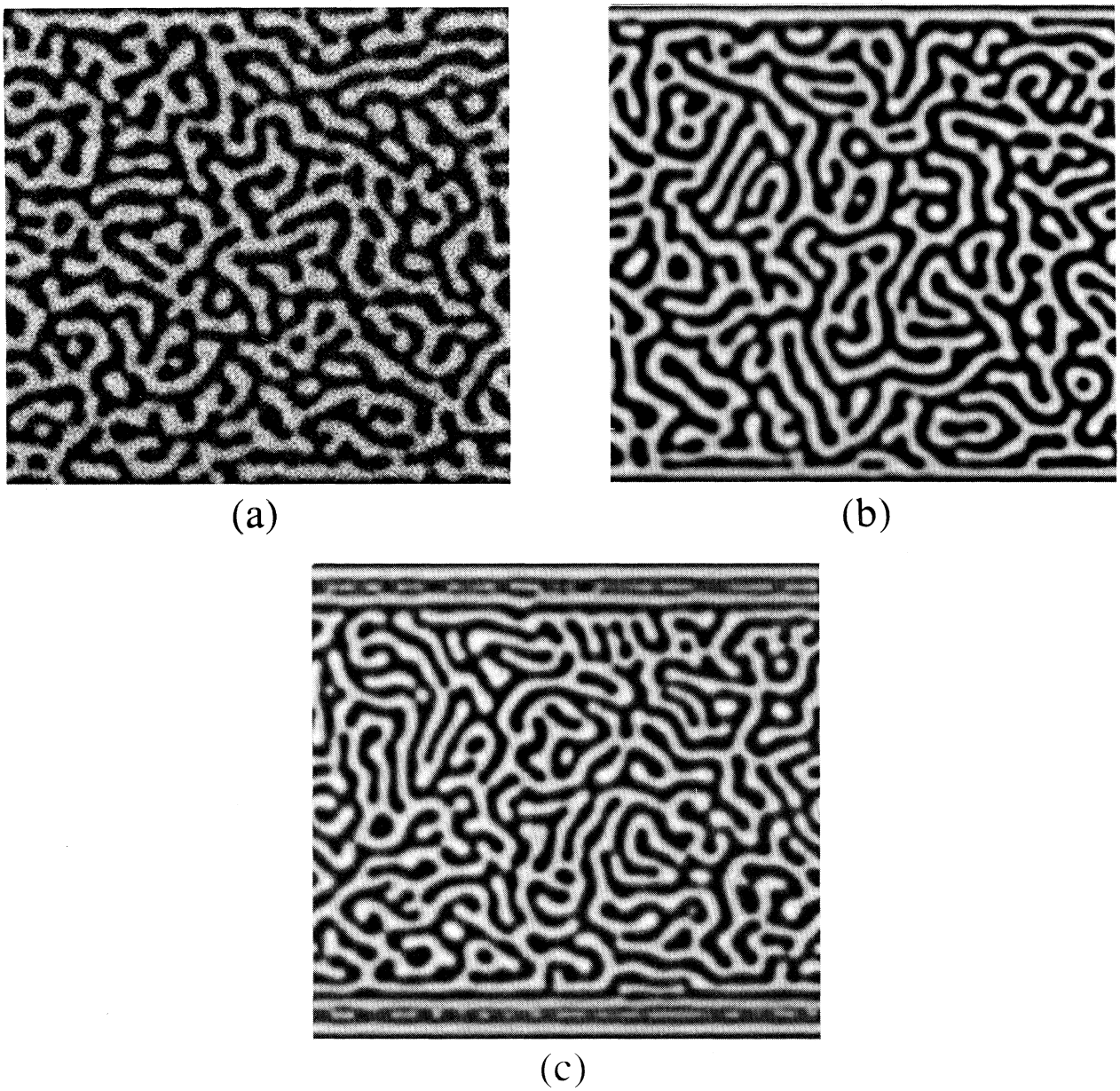

FIG. 7. Domain patterns for a single realization of δ-function surface fields of strength $H = 0.2$ and noise strength (a) $G = 10^{-2}$, (b) $G = 10^{-4}$, and (c) $G = 10^{-8}$, at time $t = 1024$. System size is 256^2. As the noise strength is reduced, concentration waves form out to larger distances, and require longer times to be replaced with a single surface domain in contact with a disordered bulk pattern.

a hemispherical protrusion from a planar interface: the small droplet is centered at $\mathbf{x} = \mathbf{0}$ and has a radius $r(t)$; the free surface of the surface domain is at $z = 0$ and the solid substrate is at $z = -h$: Fig. 10(a) shows the geometry. The flows that incorporate this droplet into the large domain may be represented by flows describing a "source" at $\mathbf{x} = -(r/2)\hat{\mathbf{z}}$ and an equal "sink" at $\mathbf{x} = (r/2)\hat{\mathbf{z}}$. For incompressible flow, the divergence of the velocity field is

$$\nabla \cdot \mathbf{v}(\mathbf{x}) = f[\delta^3(\mathbf{x} + r\hat{\mathbf{z}}/2) - \delta^3(\mathbf{x} - r\hat{\mathbf{z}}/2)]. \quad (38)$$

The amplitude f is just the amount of fluid transported from the small droplet into the large domain per unit time, or the rate of change of volume of the small droplet: $f = 2\pi r^2 dr/dt$.

Solving $\nabla^2 v = 0$ gives us a "dipolar" flow with velocity field

$$\mathbf{v}(\mathbf{x}) = -\frac{fr}{2\pi}\mathbf{D}(\mathbf{x}),$$
$$\mathbf{D}(\mathbf{x}) \equiv \frac{\hat{\mathbf{z}} - 3(\hat{\mathbf{z}} \cdot \hat{\mathbf{x}})\hat{\mathbf{x}}}{x^3}, \quad (39)$$

where only the first-order term in the droplet size r is retained. In order to take into account the capillary forces, I use an energy balance argument to relate the energy

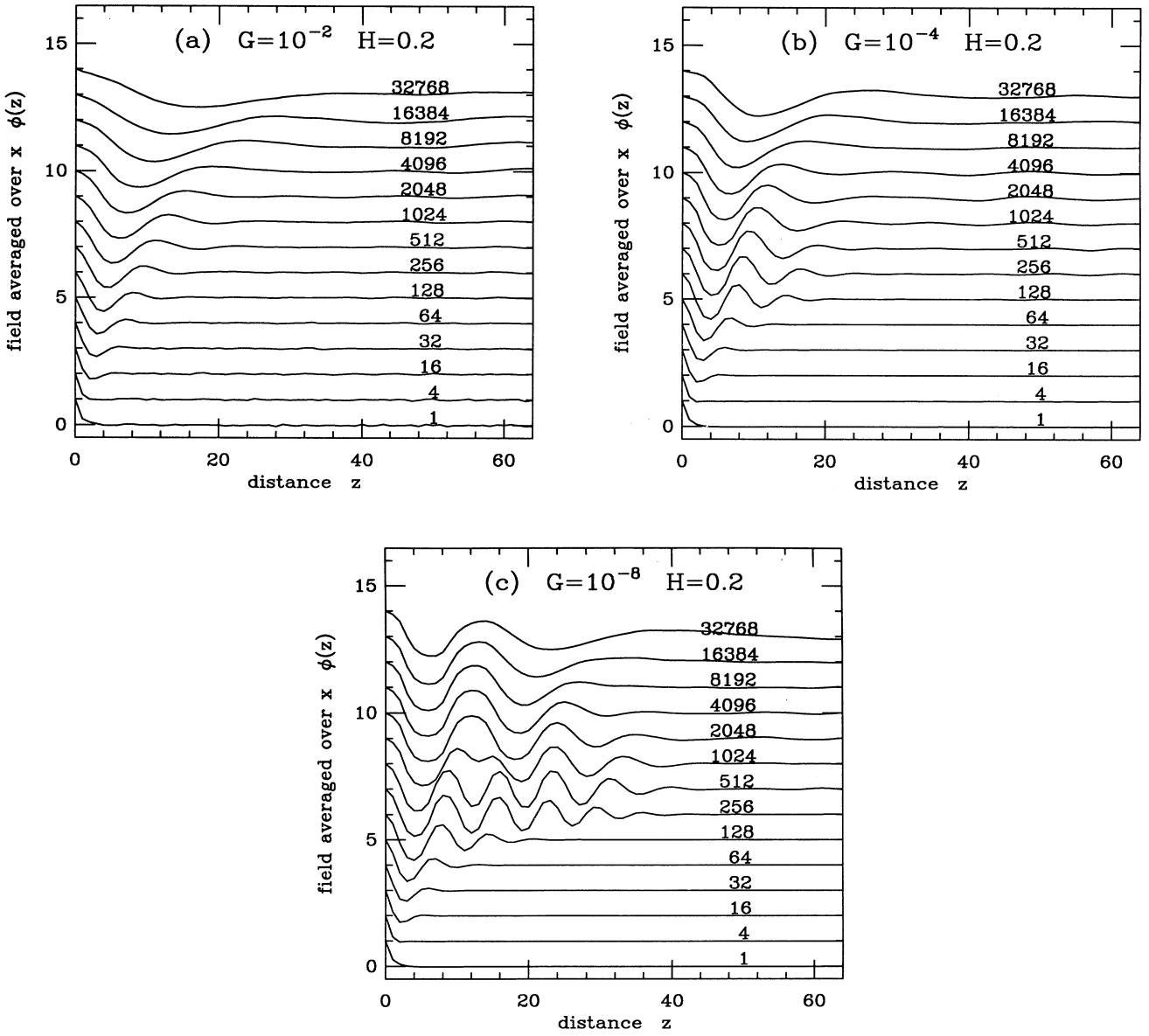

FIG. 8. Concentration as a function of distance from the wetting surface for various times: averaging has been done over the x coordinate and over six runs. Again, the three cases considered have $H = 0.2$, and (a) $G = 10^{-2}$, (b) $G = 10^{-4}$, and (c) $G = 10^{-8}$.

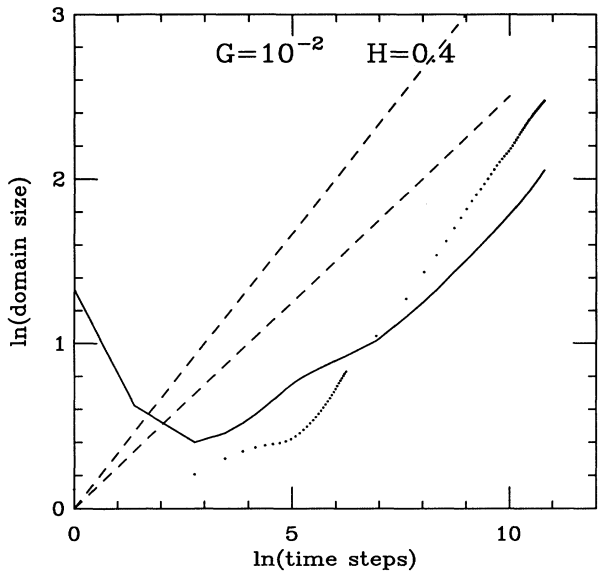

FIG. 9. Domain growth for the case $G = 10^{-2}$ and $H = 0.4$; $h(t)$ is indicated by the solid line, $R(t)$ by dots, and dashed lines indicate the power laws $t^{1/3}$ and $t^{1/4}$. Compared with Fig. 5(a), we see that the larger H in this case causes the surface domains to thicken more slowly at late times than the bulk domains.

dissipation with the rate that the interfacial energy is depleted. The rate at which energy is dissipated by the flow is

$$\partial_t E_{\rm visc} = -2\eta \int_{|x|>r} d^3x \sum_{i,k} \left(\frac{\partial v_i}{\partial x_k}\right)^2. \tag{40}$$

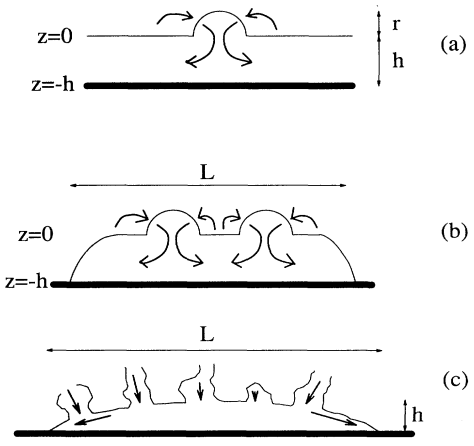

FIG. 10. Geometry of capillary flows from bulk domains into surface domains: (a) A single bulk domain is adsorbed by a surface domain of transverse dimension much larger than the bulk domain size. The surface domain boundary is located at $z = 0$, the substrate is located at $z = -h$, and the bulk domains are presumed to be of typical size $r(t)$. (b) Many bulk domains of size r flowing into a surface domain of transverse dimension L and thickness h. (c) Spreading of a surface domain in contact with random bulk domains.

This integral is cut off at $|x| < r$ since the flows at short scales are smooth and only have this dipolar character at longer length scales.

Rescaling lengths by r reduces the dissipation rate to

$$\partial_t E_{\rm visc} = -\frac{\eta f^2 C}{2\pi^2 r^3}, \tag{41}$$

where I have defined the constant of order unity

$$C = \int_{|x|>1} d^3x \sum_{i,k} (\partial_{x_k} D_i)^2. \tag{42}$$

Equating (41) with the rate of change of interfacial energy $\partial_t E_{\rm surf} = 4\pi\sigma r dr/dt$, I find

$$\frac{dr}{dt} = -\frac{2\pi}{C} v_0. \tag{43}$$

The rate of change of the small bubble radius is of order of the interface velocity for bulk hydrodynamic coarsening $v_0 = \sigma/\eta$. The transverse velocities in the large domain a distance r away from $\mathbf{x} = 0$ are also of order v_0 as this draining proceeds.

C. Many bulk domains draining into a surface domain

The same basic scaling applies to the draining of a large number of small domains of size r into a roughly flat interface, the situation experimentally encountered. Suppose that the small domains are distributed with an areal density of $\rho_a = 1/r^2(t_0)$ over a surface domain of radius L in the $z = 0$ plane, where t_0 is an arbitrary time after a quench. The geometry is shown in Fig. 10(b).

Using superposition of the single-domain flows of the preceding subsection, the velocity field is

$$\mathbf{v}(\mathbf{x}) = r f \rho_a \int_{|x|<L} d^2x' \mathbf{D}(\mathbf{x} - \mathbf{x}'), \tag{44}$$

where $f = 4\pi r^2 dr/dt$ as before. Above this dipole sheet, the velocity field decays away as

$$\mathbf{v}(z) \approx \hat{\mathbf{z}} \frac{r f \rho_a}{z}, \tag{45}$$

and thus the total dissipation is of order

$$\partial_t E_{\rm visc} = -\eta L^2 f^2 r^2 \rho_a^2 \int_{z>r} \frac{dz}{z^4}. \tag{46}$$

This leads to an estimate of $\partial_t E_{\rm visc} \approx -\eta L^2 f^2 \rho_a^2 / r$. This should be equated to the total rate of change of the interfacial energy: $\partial_t E_{\rm surf} \approx \sigma \rho_a L^2 r dr/dt$, which gives

$$\frac{dr}{dt} \approx -\frac{v_0}{\rho_a r^2}. \tag{47}$$

The transverse velocity near the edge of the surface domain is thus of order

$$v_{\|} \approx r f \rho_a \int_{r<|x|<L} \frac{d^2x}{x^3}. \tag{48}$$

Since this integral converges for $L \to \infty$, I conclude that

$v_{\|} \approx f\rho_a \approx v_0$. Thus the transverse velocities are independent of the size $r(t=0)$ of the small domains and also are independent of any characteristic transverse size L of the surface domain.

D. Flow slowing by dissipation due to proximity of substrate

The preceding discussion ignores the effect of the substrate, on which the velocity must vanish. As long as the thickness h of the surface layer is larger than the size r of the domain that is being absorbed, the preceding estimates are dimensionally correct. However, if $h < r$, there is a large contribution to dissipation from the velocity gradient required to satisfy the boundary condition. For a single domain, the dissipation due to flows above $z = h$ follows from (41); in the region between $z = h$ and $z = 0$ we estimate a velocity gradient of order $(dr/dt)/h$. Integrating this over a region of width r and height h the total dissipation rate is obtained:

$$\partial_t E_{\rm visc} = -\eta r \left(\frac{dr}{dt}\right)^2 \left(1 + \frac{r}{h}\right). \tag{49}$$

Equating this to the rate of change of interfacial energy, I obtain

$$\frac{dr}{dt} = -\frac{v_0}{1 + r/h} \tag{50}$$

as the estimate of the characteristic velocity of the draining process. For $h < r$, the flows are greatly slowed down to velocities of order $v_0 h/r$; for $h > r$, the velocities are of order v_0.

All of the above results satisfy the (entirely differently derived) scaling result of Guenoun, Beysens, and Robert [17] that the growth laws for the parallel and perpendicular dimensions of domains in contact with a interface are the same. In the present work, this arises simply because of the dipolar nature of the incompressible flow fields that incorporate the bulk domains into the puddles.

E. Spreading of domains in contact with a surface

A final effect that may lead to an acceleration of the rate of growth of L is the spreading of surface domains driven by the surface tension difference $\sigma_{1,s} - \sigma_{2,s}$. Under a wide variety of circumstances, if one of the phases completely wets the substrate then there is a universal relation ("Tanner's law") [1] between the three-phase contact line velocity v and the apparent or dynamic contact angle θ:

$$v = v_0 T(\theta). \tag{51}$$

The function T is universal and behaves as θ^3 for small θ; $T(\pi) = +\infty$. Remarkably, there is no dependence on $\sigma_{1,s} - \sigma_{2,s}$: this is due to the large amount of dissipation at the contact line, which limits the velocity to order v_0.

This law may be used to examine whether droplet spreading may play a role in accelerating the size of droplets in contact with a wetting substrate, while being in contact with a bulk spinodal pattern which is enlarging the droplet. I suppose that the droplet width is L, its thickness is h, and that the droplet volume $V = hL^2$ is being increased per unit time as

$$\frac{dV}{dt} = v_0 L^2. \tag{52}$$

This corresponds to continuous operation of hydrodynamic flows incorporating the wetting phase into the droplet: the geometry is indicated in Fig. 10(c). The contact line velocity is just dL/dt, while $\theta = \tan^{-1} h/L$:

$$\begin{aligned} \frac{dh}{dt} &= v_0 \left[1 - \frac{h}{L} T\left(\tan^{-1} h/L\right)\right], \\ \frac{dL}{dt} &= v_0 T\left(\tan^{-1} h/L\right). \end{aligned} \tag{53}$$

The two terms on the right-hand side of the first equation in (53) indicate, respectively, the effects of flows into the droplet from above and spreading flows parallel to the substrate. These equations have the scaling solutions $h(t) = Av_0 t$ and $L(t) = Bv_0 t$, for constants A and B of order unity. Thus, under the most favorable conditions for droplet growth, namely spreading of droplets being "inflated" by flows from nearby bulk domains, I find $dL/dt \approx dh/dt \approx v_0$, and thus $L \approx h \approx v_0 t$.

VI. EXPERIMENTS

A. Phase ordering of polymer mixtures

The reader may be skeptical about the possibility of observing the effects discussed in Secs. II–IV, as they require low-noise conditions and observation at small times and distances. However, experiments on phase ordering of polymer mixtures have recently made feasible such studies.

The equilibrium parameters of the free energy (1) have the following dependences on the degree of polymerization N for polymer melts [18]:

$$\varepsilon \approx (T/T_c - 1)/(Nb^d), \quad u \approx 1/(Nb^d), \quad c \approx 1/b^{d-2}, \tag{54}$$

where b is the monomer scale (of order 5 Å). The factors of $1/N$ reflect the reduction of translational entropy of a polymer, relative to that of disconnected monomers. The transition temperature T_c is itself proportional to $1/N$ since the repulsive energy between unlike monomers is unaffected by the chain connectivity. The noise strength of the rescaled model (8) is therefore

$$g = N^{-(d-2)/2} |1 - T/T_c|^{-(4-d)/2}. \tag{55}$$

For $d = 3$, $g = 1/\sqrt{N|1 - T/T_c|}$ and thus nonclassical critical behavior will be seen only in the narrow temperature range [19] $|1 - T/T_c| < 1/N$.

Recent experiments by Bates and Wiltzius [20] on bulk spinodal decomposition had $N \approx 3000$, $T_c \approx 335$ K, and $T = 300$ K, yielding $g \approx 0.06$. Such experiments are attractive also because the slow diffusion of the entangled polymers allows early times to be observed. In the above experiment, the diffusion constant for concentration fluc-

tuations ($D = kTM\epsilon$ in the unrescaled theory of Sec. I) was of order $D \approx 10^{-15}\text{cm}^2/\text{sec}$. Since the correlation length is of order the coil size ($\xi \approx 100$ Å), the scale for early times is $\xi^2/D \approx 10^3$ sec.

B. Measurements of concentration oscillations near a surface

Experiments by Jones *et al.* [21] have been done on a similar mixture in contact with a planar interface that attracted one of the components. The evolving structure was studied with forward-recoil energy-loss spectroscopy, which allowed a direct measure of the order parameter averaged over the interface plane as a function of height [$\phi(z)$ of Sec. V], with resolution of 100 Å. The polymer mixture was a blend of $N = 2300$ poly(ethylenepropylene) (PEP) and deuterated PEP (*d*-PEP) at critical composition, with T_c =365 K. Two quenches were made, to T =310 and 350 K; I estimate $g = 0.05$ and 0.10 for these two runs. In both runs, a damped oscillating $\phi(z)$ was seen to form and then coarsen in a process similar to that discussed in Sec. V.

The coil size of the polymers was of order $R_g = (N/6)^{1/2}b \approx 100$ Å: the coherence lengths are thus $\xi \approx R_g/\sqrt{1 - T/T_c} = 260$ and 491 Å. In comparison, the initial inverse wave number of the structure (of order ξ) was experimentally determined to be 250 and 475 Å. Precise values of the effective diffusion constant are not reported: I estimate $D \approx 10^{-13}(1 - T/T_c)$ cm^2/sec $= 1.5 \times 10^{-14}$ and 4×10^{-15} cm^2/sec.

The polymer mixture in this experiment was an 8000-Å-thick layer with one face in contact with a silicon substrate and the other in contact with vacuum. The free surface attracts *d*-PEP, while the Si interface attracts PEP. I estimate the rescaled surface field of Sec. II using (54): $s_B^{(1)} = N^{1/2}(1 - T/T_c)^{-1}\sigma^{(1)}b^2$. The unknown quantity $\sigma^{(1)}$ is of order of the difference in surface tension (in energy units of kT) between pure PEP and *d*-PEP at the surfaces: the surface tension difference [22] is 10^{-1} dyne/cm, giving $\sigma^{(1)}b^2 \approx 5 \times 10^{-3}$. Thus $s_B^{(1)} \approx 1.5$ and 2.5, and thus there should be complete wetting in equilibrium, as is observed experimentally.

Therefore, $\sqrt{g}/s_B^{(1)} \approx 0.15$ and 0.13 for the deep and shallow quenches, respectively: both quenches are slightly inside the plating region of Fig. 5(b). This conclusion is supported by the measurements of $\phi(z)$ reported for the deep quench [21]: the volume fraction at $z = 0$ of the preferred phase saturates rather quickly at a value less than 1, and the first minimum in $\phi(z)$ is not saturated, behavior similar to that of Fig. 8(a) ($g \approx G = 0.01$, $s_B^{(1)} \approx H = 0.2$).

At late times (10^5 sec) the oscillations in $\phi(z)$ were seen to coarsen at a rate similar to that observed in different measurements of bulk growth [approaching $R \approx (D\xi t)^{1/3}$ at late times]. However, at these late times, the concentration oscillations from *both* surfaces begin to interact, a situation that I have tried to avoid in the simulations in order to study the coarsening of a single wave in contact with random bulk domains.

C. Measurement of transverse structure of bulk and surface domains

I now consider experiments of Cumming *et al.* [23], which complement those of Jones described above, being light scattering experiments with scattering wave vector *in the plane* of the wetting substrate. The mixture was $N = 29$ polyisoprene (PI) and $N = 78$ PEP at critical composition. A cell of thickness 500 μm was used: the cell walls are transparent to the laser beam, and were completely wet by the PEP-rich phase for all of the annealing temperatures studied. By using a video camera in the scattering plane, the experimenters were able to follow the transverse structure factor with time resolution of ≈ 10 sec.

Quenches were made through $T_c = 310$ K, but in contrast to the previously described experiments, the final temperature was *at most* 1 K below T_c. Using $N = 40$, $g > 2.5$ for all of these experiments: mean-field estimates for ξ or σ will be wrong. Fortunately, Bates *et al.* [24] have carefully characterized an almost identical mixture ($N = 29$ PI, $N = 73$ PEP at critical composition). The critical temperature was $T_c = 311$ K, and nonclassical static and dynamic critical behavior was found (in the one-phase region) below $T_x \approx 340$ K (where $g \approx 0.5$). The experiments of Cumming *et al.* are deep inside the fluctuation region, and so $\xi \approx \xi_0(1 - T/T_c)^{-\nu}$ with the 3d Ising exponent $\nu = 0.63$.

Using $N = 40$ and $b = 5$ Å, $\xi_0 = (N/6)^{1/2}b = 13$ Å. The diffusion constant for concentration fluctuations is $D \approx kT/6\pi\eta\xi$: the viscosity is $\eta = 4$ poise, which gives $D \approx 5 \times 10^{-9}(1 - T/T_c)^{0.63}$ cm^2/sec. Early times are before a time $t_e = \xi^2/D \approx 3 \times 10^{-6}(1 - T/T_c)^{-1.89}$ sec, which is only 6 sec for the shallowest quenches ($T_c - T = 0.15$ K). The surface tension between the two phases is of order $\sigma \approx kT/\xi^2 \approx 2.5(1 - T/T_c)^{1.26}$ dyn/cm. The mass density of the mixture is roughly 1 g/cm^3.

I estimate a diffusive growth law (cgs units):

$$R_d(t) = (D\xi t)^{1/3} \approx (6 \times 10^{-16}t)^{1/3}. \tag{56}$$

We note that R_d is independent of the quench depth. The characteristic hydrodynamic velocity (cm/sec) is

$$v_0 = \frac{\sigma}{\eta} \approx 0.7(1 - T/T_c)^{1.26}. \tag{57}$$

Hydrodynamic coarsening will not begin until times of order $t_h \approx 30t_e$: the rationale is that the domains should be at least a few ξ thick, and concentrations should be near their equilibrium values in the domain interiors in order for surface-tension-driven flows to occur [5]. The growth law including hydrodynamic effects for $t > t_h$ is

$$R_h(t) = R_d(t_h) + Cv_0(t - t_h), \tag{58}$$

with a prefactor C which has been observed to be roughly $C = 0.1$ [20]. Such a growth law could be supposed to describe either bulk, or surface coarsening, as discussed in Sec. V.

In Fig. 11 data from the experiments of Cumming *et al.* [23] are shown: the symbols show the logarithm of wave number where a peak was observed in the light scattering structure factor, versus logarithm of time, for quenches

of 0.15, 0.35, 0.65, 0.75, and 0.95 K below the critical point. As can be seen from the data, for the two shallowest quenches, a rather slow growth (approximately $t^{1/3}$ at late times) was observed, while for the two deepest quenches, a much faster growth law was seen: the experimenters estimate $t^{3/2}$ growth. For the quench of 0.65 K, both diffusive and fast growth were observed simultaneously. By measuring the growth rate of peak intensity with time, the experimenters concluded that the slow growth applied to the bulk of the sample, while the fast growth applied to only a ≈ 10 μm-thick region, presumably at the cell walls. Microscopy also suggests that the fast ordering occurs within 10 μm of the cell window and that the length scale in the bulk corresponds to the peak showing slow growth at late times. Finally, the ratios of the two peak scattering intensities at 800 sec after the 0.65-K quench are consistent with the fast peak being the result of a region of order 10 μm thick, and the slow peak being due to scattering from domains occupying the remaining 500 μm of "bulk."

Also shown are the logarithms of the wave numbers associated with periodicity with wavelengths $2R_d$ and $2R_h$, $\pi/R_d(t)$ (dashed line) and $\pi/R_h(t)$ (solid curves), for various $1-T/T_c$ at times beyond t_h. The prefactor of the observed $t^{1/3}$ growth law within a factor of 2 of the estimate R_d. The experimental data for the bulk growth show a trend toward faster growth for deeper quenches not present in R_d: interestingly, this effect is more pronounced at earlier times.

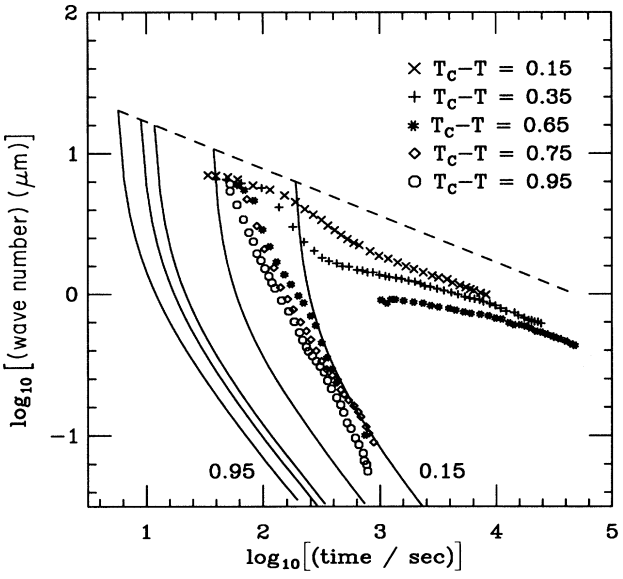

FIG. 11. Comparison of fast and slow growth measurements [23] with estimated diffusive and hydrodynamic growth laws $R_d(t)$ and $R_h(t)$. Plotted is logarithm of inverse length (wave number of peak of observed scattering in the experimental case) in inverse micrometers versus logarithm of time after quench in seconds. Experimental data for quenches of 0.15, 0.35, 0.65, 0.75, and 0.95 K are plotted along with logarithms of the wave-number estimates π/R_d (dashed line) and π/R_h (solid lines) for the same quench depths. For each quench, R_d and R_h meet at times t_h (our estimate of the time when hydrodynamic coarsening becomes possible); deeper quenches have earlier values of t_h. We observe that in each case, the experimental fast growth never exceeds R_h; the experimental slow growth rates are comparable with R_d, although they have a dependence on quench depth not predicted by the scaling result of Sec. III.

For the three deepest quenches, the experimentally observed rapid growth never exceeds our estimate for R_h, in agreement with the arguments in Sec. V suggesting v_0 as a limiting interface velocity. The fast growth is consistent with growth *slower* than the hydrodynamic coarsening observed in bulk experiments [20].

Why is $t^{1/3}$-law bulk growth observed in the three shallow quenches? At critical composition, linear growth is expected for bulk domains. However, the argument leading to this result assumes a uniform ordering structure: it is possible that in these experiments, the imbalance in composition induced by the surface is sufficient to disconnect domains so that hydrodynamic coarsening cannot proceed. Recent experiments by Jayalakshmi, Khalil, and Beysens [25] have observed a surprisingly sensitive dependence of growth laws on concentration. They have studied a fluid mixture with a concentration gradient of order 0.02/mm. Under this kind of gradient, fast growth is observed *only* in a range of concentrations of order 0.025, for quenches of 0.01–0.04 K.

I note that there is a suggestion in Cumming's 0.35-K data that hydrodynamic coarsening begins to operate at about 100 sec, but then ceases at roughly 1000 sec. This suggests an explanation of why the late-time diffusive coarsening is faster for deeper quenches, as hydrodynamic coarsening can occur earlier for the deeper quenches, as is evident from our estimates of t_h in Fig. 11.

Shi and Cumming [26] recently observed fast surface growth in a low-molecular-weight binary mixture (guaiacol and hydrated glycerol) that is known to have Ising critical behavior. The various physical quantities and consequent growth rates were comparable to the PEP-PI experiment, but better temperature control was achieved. Deep quenches produced fast surface growth with a growth law consistent with $t^{3/2}$. However, the shallowest quenches (for which the origin of time is best determined) showed surface domain size to grow roughly linearly with time, while diffusive bulk growth was simultaneously observed.

In a different binary fluid mixture, Guenoun, Beysens, and Robert [17] have observed very-late-time domain growth near a wetting substrate. Bulk domains were seen to increase in size linearly with time, while the transverse and perpendicular scales for surface domains were observed to grow at rates comparable to that of the bulk, but with a growth law of $\approx t^{0.6}$. There is no theoretical explanation of the latter exponent.

CONCLUSION

I have outlined the physical scales relevant to spinodal decomposition of a mixture near an interface that attracts one of the pure components. Immediately after a relatively deep quench, a flat surface domain forms in contact with the surface for sufficiently low-noise condi-

tions. Because of the sensitivity of the unstable mixture after the quench, surface fields much weaker than those required for complete wetting in equilibrium can lead to an ordering morphology with no domain walls contacting the surface. This may be of practical use in the deposition of microscopically thin layers of a material onto a substrate under nonwetting conditions.

The transition from this kind of morphology to droplets in contact with the substrate occurs in the nonlinear theory (studied with simulations) for surface field to noise ratios in agreement with our scaling arguments. I have discussed relevance to experiments on polymer mixtures, where the noise strength (equivalently the fluctuation region near the phase transition) is small due to the supression of concentration fluctuations by the chain connectivity.

The phenomenon originally reported by BE [4] and later observed experimentally [21] of concentration oscillations extending into the bulk from the substrate has been observed. The case where the surface field is the symmetry-breaking element in the model has been studied here; a front is observed to propagate into the bulk and is eventually halted by collision with ordering randomly oriented bulk domains. Since bulk domain growth is triggered by thermal fluctuations, the concentration oscillations penetrate a distance that is dependent on thermal noise strength [4]. However, it must be noted that for more than one or two oscillations to be observed, the effective noise strength must be extremely low due to the logarithmic dependence of the width of the surface-ordered zone on g.

At later times, the bulk and surface domains will grow, and I have measured the growth of lengths characterizing the domains. The bulk domains approach a $t^{1/3}$ growth law under a variety of circumstances, as one expects from a scaling calculation. Surface droplets, which have essentially the same structure, are observed to thicken at nearly the same rate. However, plated structures with a series of concentration oscillations thicken much more slowly than do the bulk domains. The surface domain does not coarsen appreciably until the concentration waves are destroyed by the invading bulk domains.

A scaling analysis of later times, when hydrodynamic flows may be driven by surface tension, suggests that bulk and surface domains should not differ greatly in growth rates, although dissipation in the surface layer may slow its growth over that of the bulk. The diffusive and hydrodynamic growth rates are comparable to the "slow" and "fast" growth observed in recent experiments. However, it is unclear what length of time is required for relaxation of the droplet configuration to equilibrium under conditions of partial equilibrium wetting, how that time depends on noise strength and surface fields, and how flows affect this relaxation.

Recent experiments [17] indicating a very sensitive dependence of growth law on concentration are not understood. Our understanding of how hydrodynamic flows affect coarsening at later times is still at a primitive stage. An analytical approach to these problems is needed; perhaps the recent approach of Mazenko to nonconserved [27] order-parameter growth can be applied to these problems. Boundary effects have been explored in the nonconserved case [28], but only bulk ordering has been studied in the conserved case [29]. Efforts on addition of Stokes flow to phase-ordering simulations [30] are promising and could be used to study the droplet-surface flows discussed in Sec. V.

On the experimental side, one can imagine examining larger swaths of the thermal-noise–surface-interaction space, in order to examine the droplet-plating transition. To this end, one can reduce g further (it is already surprisingly small in current experiments [20, 21]) by using larger-N polymers, although high viscosity and low diffusion constants will quickly limit how high N can be pushed. Quench depth is a useful parameter, as the noise and the effective surface field have different $1 - T/T_c$ dependence.

As mentioned in the text, current experiments on concentration oscillations have been done in rather thin samples; it would also be interesting to observe these phenomena in thick samples, in order to see the interactions between the ordered surface structure with the random bulk pattern. At late times, the invasion of the waves by the bulk domains, and under partial wetting conditions, the decay of the plated structure to surface droplets are phenomena of interest.

Scattering experiments could allow determination of the appearance of contact lines on the free surface if a probe was used that did not penetrate into the sample. Finally, it would be interesting to carry out experiments similar to those of Cumming and co-workers [23, 26] on longer polymers such as those studied by Bates and Wiltzius [20] in order to determine whether the fast surface ordering takes place under classical fluctuation conditions.

ACKNOWLEDGMENTS

I thank A. Cumming, A. Dai, E. Kramer, G. F. Mazenko, L. Norton, E. D. Siggia, B. Widom, and P. Wiltzius for their useful suggestions and comments. This work was supported by the MRL Program of the National Science Foundation under Grant No. DMR-9121654.

[1] P. G. de Gennes, Rev. Mod. Phys. **57**, 827 (1985).

[2] S. Dietrich, in *Phase Transitions and Critical Phenomena*, edited by C. Domb and J. Lebowitz (Academic Press, London, 1987), Vol. 12; M. Schick, *Les Houches, Session XLVIII, 1988, Liquides aux Interfaces/Liquids at Interfaces*, edited by J. Charvolin, J. F. Joanny, and J. Zinn-Justin (Elsevier, Amsterdam, 1990).

[3] J. D. Gunton, M. San Miguel, and P. S. Sahni, in *Phase Transitions and Critical Phenomena*, edited by C. Domb and J. Lebowitz (Academic Press, London, 1983), Vol. 8.

[4] R. C. Ball and R. L. H. Essery, J. Phys.: Condens. Matter **2**, 10 303 (1990).
[5] E. D. Siggia, Phys. Rev. A **20**, 595 (1979).
[6] If the final temperature is inside the Ginzburg region ($\sqrt{g} > 1$), the bulk and surface phase transitions will be strongly shifted from the locations predicted by mean-field theory. On top of this, the kinetic coefficient M will be strongly shifted from its "bare" value.
[7] M. Grant, M. San Miguel, J. Vinals, and J. D. Gunton, Phys. Rev. B **31**, 3027 (1985).
[8] J. W. Cahn, J. Chem. Phys. **66**, 3667 (1977).
[9] E. Brezin and S. Leibler, Phys. Rev. B **27**, 594 (1983).
[10] F. Lui and N. Goldenfeld, Phys. Rev. A **39**, 4805 (1989); W. van Sarloos, *ibid.* **37**, 211 (1988).
[11] G. F. Mazenko, O. T. Valls, and P. Ruggiero, Phys. Rev. B **40**, 384 (1989).
[12] D. A. Huse, Phys. Rev. B **34**, 7845 (1986).
[13] A $t^{1/3}$ law for thickening of a sintered crust was first discussed in I. M. Lifshitz and V. V. Slyozov, J. Chem. Solids **19**, 35 (1961).
[14] J. S. Langer, Rev. Mod. Phys. **52**, 1 (1980).
[15] Y. Oono and S. Puri, Phys. Rev. Lett. **58**, 836 (1987); Phys. Rev. A **38**, 434 (1988); S. Puri and Y. Oono, *ibid.* **38**, 1542 (1988); A. Shinozaki and Y. Oono, Phys. Rev. Lett. **66**, 173 (1991).
[16] G. Brown and A. Chakrabarti, Phys. Rev. A **46**, 4829 (1992).
[17] P. Guenoun, D. Beysens, and M. Robert, Phys. Rev. Lett. **65**, 2406 (1990).
[18] P. G. de Gennes, *Scaling Concepts in Polymer Physics* (Cornell University Press, Ithaca, 1985).
[19] P. G. de Gennes, J. Phys. Paris **38**, L441 (1977).
[20] F. S. Bates and P. Wiltzius, J. Chem. Phys. **91**, 3258 (1989).
[21] R. A. L. Jones, L. J. Norton, E. J. Kramer, F. S. Bates, and P. Wiltzius, Phys. Rev. Lett. **66**, 1326 (1991).
[22] L. Norton (private communication).
[23] A. Cumming and P. Wiltzius, Phys. Rev. Lett. **66**, 3000 (1991); A. Cumming, P. Wiltzius, F. S. Bates, and J. H. Rosedale, Phys. Rev. A **45**, 885 (1992).
[24] F. S. Bates, J. H. Rosedale, P. Stepanek, T. P. Lodge, P. Wiltzius, G. H. Fredrickson, and R. P. Hjelm, Phys. Rev. Lett. **65**, 1893 (1990).
[25] Y. Jayalakshmi, B. Khalil, and D. Beysens, Phys. Rev. Lett. **69**, 3088 (1992).
[26] B. Q. Shi, C. Harrison, and A. Cumming, Phys. Rev. Lett. **70**, 206 (1993).
[27] G. F. Mazenko, Phys. Rev. Lett. **63**, 1605 (1989); Phys. Rev. B **42**, 4487 (1990).
[28] G. F. Mazenko, O. T. Valls, and P. Ruggiero, Phys. Rev. B **40**, 384 (1989).
[29] G. F. Mazenko, Phys. Rev. B **43**, 5747 (1990).
[30] T. Koga and K. Kawasaki, Phys. Rev. A **44**, R817 (1992); A. Shinozaki and Y. Oono, *ibid.* **45**, R2161 (1992).

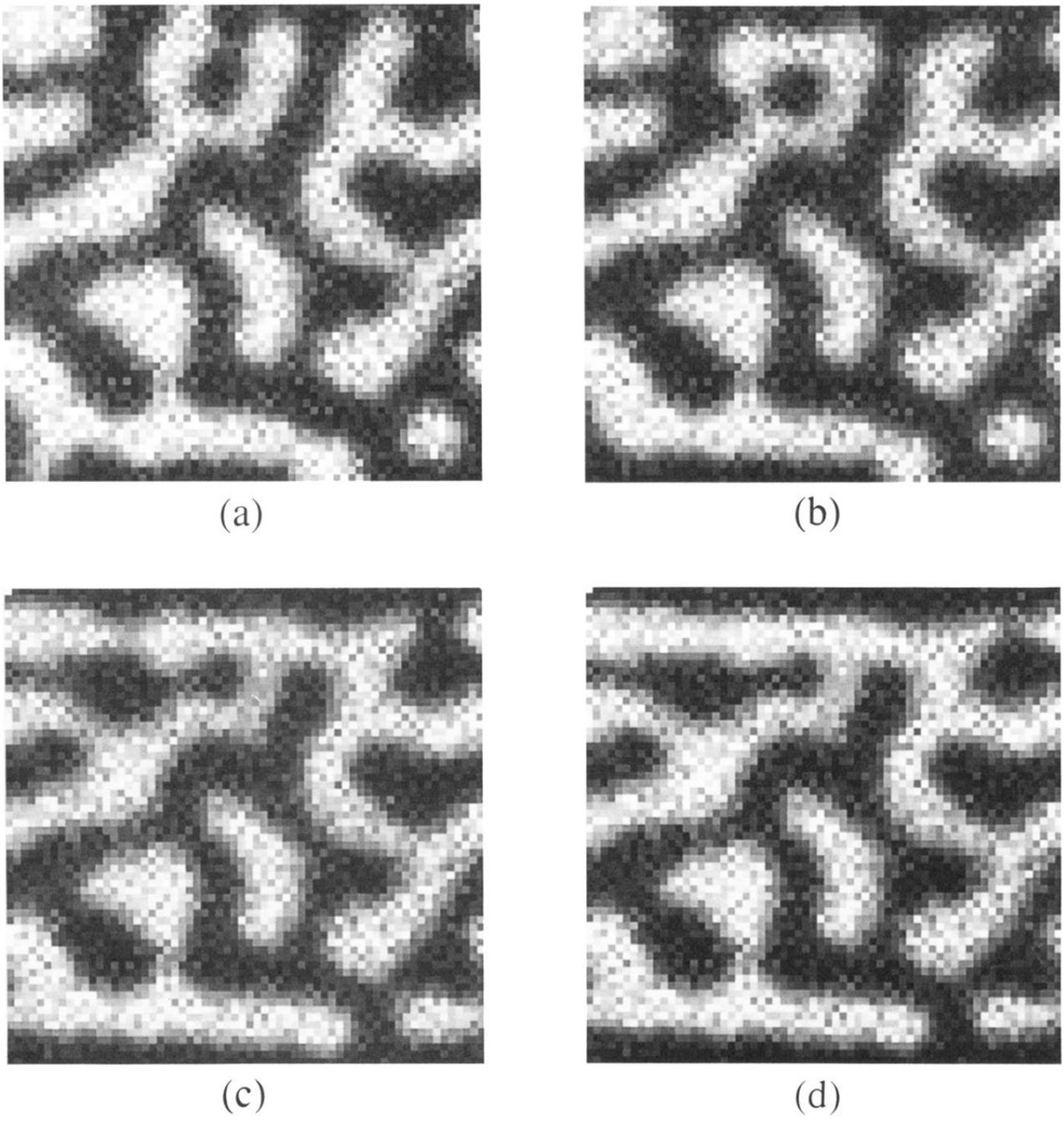

FIG. 4. Configurations of 64×64 CDS at time $t = 1024$ for $G = 0.01$ and $H = 0.1$, 0.2, 0.4, and 0.6 are shown in (a), (b), (c), and (d), respectively. The wetting surfaces are at the top and bottom of the figures. Cases (a) and (b) show surface droplets; (c) and (d) show "plating."

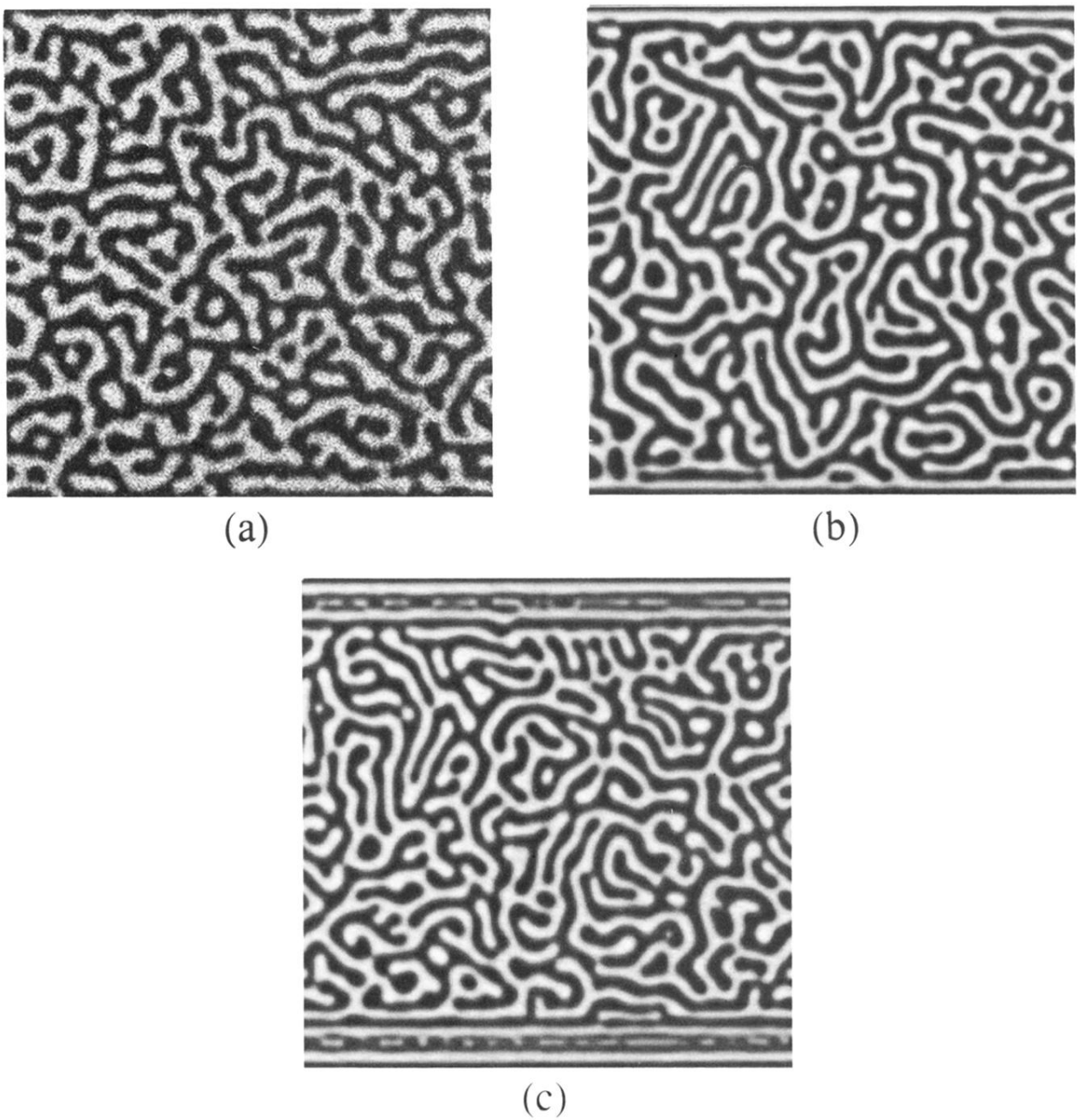

FIG. 7. Domain patterns for a single realization of δ-function surface fields of strength $H = 0.2$ and noise strength (a) $G = 10^{-2}$, (b) $G = 10^{-4}$, and (c) $G = 10^{-8}$, at time $t = 1024$. System size is 256^2. As the noise strength is reduced, concentration waves form out to larger distances, and require longer times to be replaced with a single surface domain in contact with a disordered bulk pattern.